A 3D imaging and visualisation workflow, using confocal microscopy and advanced image processing for brachyuran crab larvae

S. A. KAMANLI[1, 2, 3], T. C. KIHARA[4], A. D. BALL[2], D. MORRITT[1], P. F. CLARK[3]

[1] *School of Biological Sciences, Royal Holloway University of London, Egham, Surrey, UK*

[2] *Imaging and Analysis Centre, Core Research Laboratories, The Natural History Museum, London, UK*

[3] *Department of Life Sciences, The Natural History Museum, London, UK*

[4] *German Centre for Marine Biodiversity Research, Senckenberg am Meer, Wilhelmshaven, Germany*

Running header: 3D imaging of crab larvae using CLSM

Correspondence to: Seyit Ali Kamanli, Department of Life Sciences, The Natural History Museum, Cromwell Road, London SW7 5BD, UK. Tel: +44(0)2079425564; fax: +44(0)2079425054; e-mail: Seyit.Kamanli.2013@live.rhul.ac.uk

Key words. Confocal laser scanning microscopy, 3D imaging, Drishti, ImageJ, visualisation, brachyuran crab larvae.

Summary

Confocal laser scanning microscopy is an excellent tool for non-destructive imaging of arthropods and can provide detailed information on morphology including fine surface detail. A methodology is presented here for the visualisation by confocal microscopy of arthropods, using brachyuran crab zoeal stages as examples and post-processing techniques derived from micro-CT protocols to improve the final images. This protocol is divided into description of the pre-processing steps (cleaning, staining, digesting and mounting), confocal laser scanning microscopy and data visualisation using open-source, freeware programmes ImageJ and Drishti. The advantages of using ImageJ to standardise stack data and Drishti for surface rendering are discussed. The methodology has been comprehensively tested using data acquired from all four brands of confocal microscope (Leica, Nikon, Olympus and Zeiss).

Introduction

Confocal laser scanning microscopy (CLSM) offers an excellent option for non-destructive imaging of brachyuran crab larvae and other macro-invertebrates (Butler *et al*., 2010). The images obtained are comparable in quality to scanning electron microscopy (SEM) at the same magnifications and the technique offers a 3D data set. In addition, the sample preparation routine for CLSM is simpler than that for SEM. Applying SEM protocols to individual larval appendages (which may be only a few hundred microns in length and tens of microns in diameter) can be difficult (Wolf, 2010) and often results in them being damaged (Michels, 2007) or even lost during the preparation steps due to the fact that they are so small. Finding a suitable SEM dehydration protocol which does not result in distortion of the cuticle, particularly in larval specimens, has proven to be extremely challenging (Wolf, 2010), whereas samples are examined in a hydrated state for CLSM. This allows the appendages to be manipulated within the mounting medium to offer views of the specimen from multiple angles

which can be problematical to achieve using SEM since some viewpoints may be inaccessible due to the way that the specimen is mounted and the tilt limitations in the SEM (e.g. Fig. 1a). Since CLSM is an optical technique, the transparency of the sample allows the origins of spines/setae and internal anatomy (musculature, digestive or nervous system) to be viewed/recorded and specimens held in historical slide collections to be examined/compared with recently collected material. CLSM illustrations can include much finer details than the traditional line drawings (e.g. Fig. 1b, c) for morphological descriptions, which are incredibly time consuming (Coleman, 2006) and figuring dense concentrations of setae can be challenging. Furthermore, CSLM samples can be recovered after imaging and used for DNA extractions.

Previous studies have described a number of different techniques for applying CLSM to macro-invertebrates including the use of a variety of stains, mounting media, and cleaning protocols (Table 1). However, one issue with CLSM visualisation is that the software is optimized for generating images of transparent, fluorescent volumes rather than for rendering and lighting surfaces. Commercial software capable of producing this type of visualisation tends to be expensive. Workflows can be developed to allow the use of the open-source freeware programme "Drishti" (http://sf.anu.edu.au/Vizlab/drishti/; Limaye, 2012) to visualise CLSM data (e.g. Fig. 1d).

The purpose of this study is to demonstrate a workflow for the 3D imaging of arthropods using CLSM and visualisation using a combination of ImageJ and Drishti to process the resulting data. The first stage of the workflow, as detailed in the pre-processing section of this paper, is the application of improved cleaning, staining, digestion and mounting protocols to the specimen prior to scanning. The second stage is scanning of the specimens using a Nikon A1-Si confocal microscope. The third stage is a specific method for processing the resulting image stacks using the open source software programmes ImageJ and finally apply Drishti for

3D visualisation. The data presented here was obtained using a Nikon CLSM, however, the third stage of the workflow was also tested using comparable datasets obtained using confocal microscopes from Leica, Olympus and Zeiss. A common workflow for preparing data from different brands of confocal microscope for 3D visualisation has been created using ImageJ (http://imagej.nih.gov/ij/; Schneider *et al*., 2012) and the results were found to be consistent across all instruments tested. This method is detailed in the post-processing (3D modelling) section of this paper.

Materials and Methods

Source of larvae

Eriocheir sinensis H. Milne Edwards, 1853; ovigerous female; Tilbury, River Thames, England; collected by Roni Robbins, 16 March 1999; hatched 14−16 April 1999; Natural History Museum, London (NHM) registration number 2002.791.

Sesarma curacaoense De Man, 1892; ovigerous female; coastal mangrove swamp near Mangrove Point, Trelawny, northern Jamaica; collected March 1993 (see Anger *et al*., 1995).

Armases miersii (Rathbun, 1897); ovigerous female; Devil's Cook Room, Trelawny, Jamaica; collected Schuh & Diesel, March-July 1996 (see Cuesta *et al*. 1999).

Larvae

Pre-processing

Protocol. A number of protocols were applied to the larval specimens during the preparation of the slides, namely cleaning, staining, protein digestion, and mounting. Specimens were scanned using a Nikon A1-Si confocal microscope (Nikon Corporation, Tokyo, Japan) fitted to a Nikon Eclipse upright microscope. Generation of the 3D images was conducted using the open source software programme Drishti (version 2.6.1; Limaye, 2012). Other brands of

confocal microscopes including the Olympus Fluoview FV1000 IX81 inverted microscope (Olympus Corporation, Tokyo, Japan), Zeiss LSM 880 airy scan upright confocal microscope (Carl Zeiss, Jena, Germany), and Leica TCS SP5 (Leica Microsystems, Wetzlar, Germany) equipped with a Leica DM5000 B (upright microscope) were also tested using a protocol with the aim of finding a consistent workflow. In order to apply the same instructions to the different types of confocal image data, ImageJ was used before the application of Drishti (Fig. 2).

Cleaning. For this study, laboratory hatched larval (zoeal) stages of the Chinese mitten crab (*Eriocheir sinensis*), previously fixed in 70% ethanol and deposited in the crustacean collections of the NHM, were scanned using CLSM. Numerous zoeae were contaminated with deposits that had adhered to the exoskeleton. The specimens were cleaned (see Sewell & Cannon, 1995; McAllen & Taylor, 2001) using Decon 90 (Decon Ltd., Sussex, England). Two or three drops of Decon 90 were added to 100 ml of 70% ethanol and specimens were left in this solution for 3 to 4 hours. This solution was gently agitated occasionally by hand during the cleaning process. The sonication methodology as proposed by Felgenhauer (1987) and the use of a tumbler were also trialled. After cleaning, the specimens were pipetted into deionised water for 5 minutes and washed thoroughly including three changes of 5 minutes each. The chemistry of the deposits was also investigated using X-ray spectroscopy using a LEO 1455VP SEM (Carl Zeiss, Jena, Germany) fitted with an Oxford Instruments X-Max 80 EDX (Oxford Instruments, Oxford, England) detector (see **Supporting Information 1**; SEM preparation). The SEM was operated in variable pressure mode (15Pa chamber pressure) at 20kV and the samples examined qualitatively in spot mode using internal standards.

Staining and digestion. The larvae were stained using a 1:1 mixture of Congo red (Fisher Scientific Ltd., Loughborough, England) and acid fuchsin (Sigma-Aldrich Co. Ltd., Irvine,

England). These stains were available in powder form and each made into a stock solution by dissolving 0.5 mg of stain in 100 ml of deionised water. Stock solutions were filtered (Filtropur 0.2 µm) to remove unwanted particles. The stains were stored in a cupboard at room temperature (ca. 20° C) in dark glass vials and covered with aluminium foil to protect them from the light which causes bleaching. Before staining the specimens, Congo red and acid fuchsin stock solutions were mixed 1:1 in a glass dish using separate plastic pipettes for each stain. Using mounted needles, the larvae were carefully lifted into the mixed stain, covered with a glass lid to prevent evaporation and left in a covered box for 24 hours at room temperature. The larvae were next transferred into a solution of SDS (5.2g (0.18M) SDS (sodium dodecyl sulphate) and 0.24g (0.03M) NH_4HCO_3 (ammonium hydrogen carbonate) in 100ml deionised water) + DTT (0.1g 1, 4 dithio-DL-threitol in 5ml stock solution of SDS) to be digested (see **Supporting Information 2**; Preparation of SDS + DTT solution; Fischer & Ahlrichs, 2011). A few drops of the SDS + DTT solution (depending of the size and number of specimens) were dropped into a cavity slide. The stained specimen was placed into the solution and left until the muscles within the larvae were digested. For zoea I (ZI) larvae (Fig. 3a) this was achieved in 75 minutes. As the size increased in subsequent zoeal stages (ZII–ZVI), the duration of immersion in the SDS + DTT solution was increased depending on the stage of development, e.g. ZII (Fig. 3b) = 2−3 hours, ZIII (Fig. 3c) = 4−5 hours, ZIV (Fig. 3d) = 6−8 hours, ZV (Fig. 3e) = 10 hours, ZVI (Fig. 3f) = more than 10 hours. When digestion was complete, the larvae were rinsed three times in deionised water (each rinse lasting 5 minutes). Digested specimens were then transferred back into the mixture of Congo red and acid fuchsin where they remained for a further 24 hours in a box, at room temperature, for a final staining.

Mounting in glycerine and specimen dissection. The use of a suitable mounting medium was essential in order to deliver optimum images using CLSM and for 3D re-construction purposes.

The larvae (ZI and ZII) were removed from the stain and transferred into a solution of 10% glycerine and 90% deionised water. This solution avoided shrinkage problems when transferring the larvae from the stain to glycerine for dissection, but this solution concentration was varied according to the stage and size of the larvae e.g. 25% glycerine and 75% deionised water was used for ZIII and ZIV, and 50% glycerine and 50% deionised water was used for ZV and ZVI. Before dissection, glass slides were prepared using self-adhesive reinforcement rings (Fig. 4) glued to the surface as described by Kihara & Falavigna da Rocha (2009). Reinforcement rings raised the cover slip above the slide and allowed more space for the dissected appendages to lie naturally in the cavity without being crushed and flattened. Two to three droplets of glycerine solution were pipetted into the cavity formed by the reinforced rings.

The larvae were dissected under a Leica MZ 16 stereomicroscope (Leica Microsystems, Wetzlar, Germany) using tungsten wire needles (Clark & Cuesta, 2015). After dissection, the appendages were individually transferred into the prepared cavities of the glass slides. This ensured that the slide had a clean, debris free background for confocal microscopy. For the pleon and larger appendages, the number of self-adhesive reinforcement rings used was increased (Michels & Büntzow, 2010). After the appendages had been placed into the cavities, they were carefully covered using 0.17 mm thick coverslip. After dissection and mounting, slides were kept in a dark area at room temperature prior to scanning as Congo red and acid fuchsin are affected by light.

Confocal laser scanning microscopy

The larval appendages were scanned using a Nikon A1-Si confocal microscope. Four lasers were available, 405 nm, 488 nm, 561 nm, 640 nm. Although an excitation wavelength of 561 nm was recommended by Michels & Büntzow (2010) to match the optimal fluorescence of Congo red, a wavelength of 640 nm also proved effective. During scanning, all available

wavelengths were used so that no data were missed. For each preparation, the most appropriate objectives were chosen to match the size of the appendages.

For larger appendages, such as the pleon, a 20× dry objective with a numerical aperture (N.A.) of 0.75 was used to obtain a general image before scanning at a higher magnification. Oil immersion objectives were used to increase resolving power of the microscope for scanning at 40× with N.A. of 1.30 and 60× with N.A. of 1.4 to produce higher resolution images of smaller larval appendages. Detector gain and amplitude offset were manually adjusted to deliver a black background. Setules (fine structures with a relatively low signal level) of the appendages, proved challenging to scan. To specifically visualise the setules, the offset was increased in order to make them apparent; this would also apply to any similar fine arthropod feature (fine setae, scales etc.). For image setting, the Z-intensity correction function was used to avoid oversaturating images. This function provided an opportunity to make colour adjustments between oversaturated or under saturated layers. Optimisation of the number of Z-frames scanned was also required. 3D reconstruction required more Z-frames than 2D images, so the number of frames needed to be selected to match the final use case. Acquisition times were manually adjusted to deliver an acceptable background noise level and slides were typically scanned with 2× frame averaging. The format of all images is 1024×1024 pixels and these were viewed using maximum intensity projections as 2D image stacks.

Two options can be applied to scan large appendages at higher magnification using CLSM. The first method uses the “large images” software option of the microscope and scans the sample in discrete areas known as tiles. The large images software option automatically stiches the tile together (Fig. 5a). Scanning duration, however, increases when applying this method and the resulting data sets can be extremely large. Manipulating such data sets may present problems during post-processing unless a powerful computer is made accessible. A

second option is to scan the sample in sections (i.e. basis and endopod separately; Fig. 5b, c) and then, after applying ImageJ and Drishti, merge these using Photoshop (Fig. 5d).

Nikon confocal microscopes store the data stacks as ***.nd2 file; Leica as ***.lif; ***.oib files for Olympus and ***.czi files for Zeiss (Fig. 6). Each manufacturer provides its own software package to visualise the image and to create maximum intensity projections. FV 10−ASW 4.2 software was developed by Olympus; ZEN lite imaging software for Zeiss; LAS AF 2.2.1 software is used by Leica and NIS elements viewer (version 4.20) by Nikon.

Post-processing using ImageJ and Drishtiimport

The first method for importing image stacks into Drishtiimport involves the use of ImageJ. Instead of using the confocal manufacturer software packages, the image stacks are opened directly in ImageJ which splits the stack data into channels which can be viewed independently. At this point, the image properties (voxel size) should be noted in order to produce a scale bar later in Drishti. Any channels considered to be of insufficient quality can be ignored and the remaining channels merged. The advantage of using ImageJ is that merged channels can be converted to 8-bit composite images creating one common workflow for data from any brands of confocal microscope. The merged images can then be exported into Drishtiimport. Multi-channel data can be easily manipulated by Drishti and produce images of much greater quality (see **Supporting Information 3** & **4**; Exporting stack data into ImageJ and Importing stack data into Drishtiimport, respectively).

As an alternative method, the stack data files can be exported as TIFF images by separating the chosen excitation wave lengths (channels) using the software packages provided by the manufacturers to deliver a single image stack for each channel. Typically, only a single channel was selected for 3D modelling (Bourke, 2011). For this application, the orange channel (561nm) provided the optimal fluorescence signal for Congo red and acid fuchsin stains. All

stack images in one channel were then selected and transferred to a new folder (e.g. "Orange channel"). Image properties (voxel size) were noted for later reference in order to produce a scale bar in Drishti.

Whichever workflow was chosen, the new folder was then imported into Drishtiimport which standardises the data and creates a ***.pvl.nc file called "volumes.pvl.nc" (see **Supporting Information 4**; Importing stack data into Drishtiimport). The user has the option to individually import all the channels into Drishtiimport to be saved as volumes. Although Drishti does provide an option to load more than one volume, the size of the files can be extremely large and may prevent the programme from operating. Furthermore, any resulting images tended to be over saturated.

Visualisation of data using Drishti (*3D Visualisation*)

After opening Drishti (Lovett, 2013), the volume files (***.pvl.nc) created in Drishtiimport were imported, processed and visualised in 3D. The processing capabilities of Drishti were used as follows. Before visualising the volumes in high resolution in 3D, the images were cropped to fit the scanned image or area of interest on the appendages. Adjusting the lighting option helped to visualise the setae on the appendages. Adding a scale bar and increasing the image quality was possible using the programme. As well as visualising the surface characters on the appendages in detail, Drishti allowed the 3D specimen dataset to be reoriented and more than one snapshot of the same appendage to be taken from different angles. Consequently, the exact number of setae and other details could be accurately determined. One of the most helpful options of the programme was the ability to edit pictures by removing debris or unwanted tissues on the images in 3D. Opening the "command help" box gave a number of different options for processing the volumes e.g. making videos. The images can be adjusted and improved (see **Supporting Information 5**; Drishti visualisation instructions). Final images

were adjusted in Adobe Photoshop. Adjustments included modifying the brightness and contrast, changing the image and canvas size, improving the quality and consistency of the Drishti scale bars, standardising the background, deleting any remaining debris and saving as a final image for publication.

"Digital dissection". This may also be referred to as "data cleansing" and/or "segmentation". Unprocessed CLSM datasets frequently contained fragments of dissected debris and additional tissue which appeared to "float" in the 3D volume or which were attached to appendages. This unwanted data can be removed (cleaned) using Adobe Photoshop, but this option only affects the final 2D viewpoint of the 3D volume. Such editing may pose ethical issues with regards to alteration of the image since areas "behind" the fragment would also be removed and need to be "cloned" back into the image. A much better option was to remove the unwanted scanned fragments directly from the 3D volume using Drishti by rotating the specimen. From examination of the rotated specimen, the viewer can determine whether the fragment was a part of the specimen. If not, it can be removed to allow for an improved visualisation of the specimen. 3D volume manipulation therefore allowed for the specimen to be digitally dissected in post-processing and this was considered to be a much more powerful technique than simple 2D image manipulation (see **Supporting Information 6**; Segmentation instructions). After the 3D manipulation process, a 2D image was saved and edited in Photoshop.

Results and discussion

Cleaning and digesting

Cleaning the specimens with Decon 90 proved to be an effective method of removing debris that had adhered to the exoskeleton (compare Figs. 3 with 7a). The sonication methodology proposed by Felgenhauer (1987) for cleaning aquatic arthropods, proved ineffective as it often

resulted in the natatory setae of the maxillipeds of the zoeae becoming tangled. A similar problem was encountered when using a tumbler.

The results of the SEM-EDX analysis showed that debris found on limbs was composed of calcium carbonate (see Fig. 7a). These items of debris were effectively removed using the surface-active cleaning agent, Decon 90.

Digesting the muscle within specimens using a mixture of SDS + DTT (Fischer & Ahlrichs, 2011) was an effective method of clearing the appendages, making them more transparent and fluorescent for CLSM imaging. This clearing of internal tissue also helped the visualisation of setae that were otherwise masked behind the muscles on the distal side of the appendage. Furthermore, dissection of zoeae became much easier after the specimen had been placed in the digesting solution. Another advantage of using the digestion mixture was to balance the acquisition settings of the microscope to avoid having over/under saturated images. As the setae provided a weaker signal than the main part of the exoskeleton, the settings of the channels needed to be increased to visualise these smaller structures. If the settings were increased, however, the main exoskeleton had a tendency to become over saturated because it yielded a stronger signal (Fig. 8a). This problem was resolved by digestion since its relative signal strength was reduced compared to that of the setae (Fig. 8b).

If the appendage was not digested, however, some of the minute exoskeletal structures were "masked" (Fig. 9a) by the signal from basial musculature of the second maxilliped and did not appear when ImageJ and Drishti was applied to the confocal stack data (Fig. 9b). But after digestion of the basial muscles (Fig. 9c), these tiny structures could be visualised when fully processed (Fig. 9d).

Comparing methods to eliminate oversaturation after staining

Congo red has been a commonly used external stain for crustaceans and polychaetes (Michels & Büntzow, 2010; Michels & Gorb, 2012) prior to CLSM. Although the present study demonstrated good results using Congo red alone for CLSM, some appendages were not completely saturated by the stain (Fig. 8c). This problem of patchy staining was mentioned by Michels & Büntzow (2010) and Böhm *et al.* (2011) who were attempting to stain small crustaceans, the cuticle of polychaetes and the tarsal sensilla of Protura. Michels & Büntzow (2010) clarified that Congo red stained the exoskeleton effectively, but was not so successful for internal tissues and proteins. Böhm *et al.* (2011) attributed this to the embedding medium and compensated for this by changing acquisition settings during CLSM imaging. In order to overcome this problem in the present study, Congo red was mixed with acid fuchsin, which is another effective stain of arthropod exoskeletons. The combination of Congo red and acid fuchsin greatly improved the overall saturation of staining and proved a more effective way to balance the acquisition settings compared to using Congo red alone (Fig. 8d).

In addition, Michels & Büntzow (2010) suggested that after staining, specimens should be washed several times until the Congo red was no longer present prior to dissection. This was not found to be an issue in the present study because the specimens were removed from the stain and placed in a solution of diluted glycerine and then the appendages were dissected. The dissected appendages were then individually transferred to slides containing a fresh solution of dilute glycerine to be scanned; the specimens were thus effectively isolated from the Congo red.

Comparison of mounting media

Two types of mounting medium were initially trialled; polyvinyl lactophenol (permanent) and diluted glycerine (non-permanent). Polyvinyl lactophenol was placed on a glass slide, stained larvae were transferred directly into it, dissected and a cover-slip applied. Polyvinyl

lactophenol proved to be extremely viscous and hard when set, consequently manipulation of the appendages into an improved position for CLSM was almost impossible. An advantage of a hard setting mount was that during scanning the heat caused by the laser did not change the position of the specimen. It was not possible, however, to reposition the specimen or to use it for DNA extractions after scanning. In addition, during dissection, much debris was produced and these fragments adhered to the appendages (Fig. 7b-c) causing background noise. Furthermore, removing the debris from the appendage or background using Drishti or Photoshop proved extremely time-consuming and was not always successful (see circled areas, Fig. 7d). The background noise could be compensated for by increasing averaging times. But this could increase the duration of scanning (scan time doubled with 4 times averaging, tripled with 8 times averaging and quadrupled with 16 times averaging). Consequently, a clean background reduced the duration of scanning and helped to avoid bleaching of the stain. Another issue with polyvinyl lactophenol was it caused immediate shrinkage of the specimens that were transferred to the medium. The mountant could be diluted with alcohol to avoid specimen shrinkage, however, both polyvinyl lactophenol and alcohol, individually and together, did in time bleach the stained specimens.

Glycerine was therefore the preferred mounting medium for CLSM studies. Shrinking specimens placed in diluted glycerine could be recovered with the addition of more deionised water and, furthermore, could be easily manipulated for re-positioning. A disadvantage of this medium, especially when diluted, was that it could be heated by the lasers during scanning. There was a tendency for it to liquefy which caused movement of the specimen. Another problem was the formation of air bubbles. Their expansion during scanning caused the specimen to move and the production of a blurred final image. Air bubbles also tended to form over time and appeared overnight between mounting the specimen and scanning. This was possibly because the initial volume of fluid was insufficient or evaporation had taken place

overnight. It was therefore better to scan directly after the sample had been mounted. Furthermore, samples could also lose their stain if allowed to remain in glycerine over long periods of time.

Scanning procedures

The use of reinforced rings to create adequate space under the coverslip (Fig. 4) proved to be effective in preventing samples from being crushed and distorted. Once the sample was correctly positioned the confocal microscope was able to obtain extremely high quality image data. For larger specimens it proved necessary to tile the sample (collect data as series of overlapping fields of view in X and Y and also Z) (Fig. 10) which led to long acquisition times, with consequent risk of specimen movement. The resulting data files were also exceptionally large and processing these data using Drishti required an extremely powerful computer. This problem was also solved by scanning the appendage in separate sections and merging these at the end of the scanning procedure using Photoshop (Fig. 11), however, this protocol was somewhat time-consuming.

For smaller larval appendages, 40× and 60× oil immersion objective lenses were used to produce higher resolution images. Using a lower magnification objective lens to obtain a larger field of view was ineffective since the lower magnification lens did not provide adequate resolution to resolve fine setae (e.g. dorsal setae on somite of the pleon are not resolved with lower magnification lenses; Fig. 12). Lower magnification lenses also reduced resolution along the Z-axis and were thus not capable of obtaining sufficiently fine image slices for effective 3D reconstruction in Drishti. The requirement to obtain large numbers of Z slices and for image tiling meant that confocal microscope data acquisition was relatively slow and could take several hours, hence the need to optimise the stability of the sample in the mounting medium.

ImageJ and Drishti

The methodology and data processing workflow (Fig. 2) described here was successfully tested on confocal microscopes manufactured by Olympus, Zeiss, Nikon and Leica. The method for handling the data was the same and the ImageJ and Drishti import process was identical for each file format (Fig. 13). The final quality of merged channels images combining ImageJ and Drishti appeared to be an improvement compared to importing a single channel into Drishti (using the manufacturers' own programmes to extract each channel). Merged channel images provided more information, especially with regard to the visualisation of setae. Drishti provided an added advantage in being able to reconstruct stack data and manipulation of images.

Once 3D datasets had been acquired, Drishti proved to be a powerful tool in reconstructing the specimen from different viewpoints (Fig. 14) and also offered the advantage of allowing the user to remove parts of the specimen from the foreground to reveal features which would otherwise be obscured (a useful form of digital dissection; Fig. 14c). Various images of brachyuran crab larvae from different species (*Eriocheir sinensis*, *Sesarma curacaoense*, *Armases miersii*) were scanned using CLSM and processed with ImageJ, Drishti and Photoshop (see Figs. 15−17).

Additionally, Drishti is a freeware software programme while other comparable surface rendering packages are extremely expensive. The visualisation packages produced by Nikon, Leica, Olympus and Zeiss are limited and not cross compatible, whereas ImageJ and Drishti are universal across all brands.

Conclusions

Conventional observation of fine features, as seen in brachyuran larvae, normally relies on light microscopy often using techniques such as DIC (differential interference contrast) or phase

contrast (Fig. 18). Furthermore, dissected appendages are challenging to mount as they can move whilst trying to fix them in an appropriate position. The narrow focal depth of compound microscopes may also make some direct observations difficult, as a result features can be overlooked. Consequently, many line drawings tend to simplify and codify the essential features for diagnostic illustrations. For specimens with complex topography and setation, however, this approach can be subjective and makes comparison difficult (Fig. 1b, c). In addition, traditional 2D photography, even with the addition of focal stacking, may not accurately record the 3D complexity of limbs and larval appendages or the position of setae. In comparison, high quality CLSM image data can be further enhanced by the use of Drishti. For example, in previous studies, the number of setae on the basis of the first maxilliped especially in the small early zoea stages, such as ZI and ZII (for correct setation see Figs. 13a; 16a) and the fine second seta on the first and second segments of the first maxilliped endopod were overlooked (for correct setation see Figs. 13b; 16b). In addition, one seta can mask another if it lies along the same image path, but on a different focal plane. The masked setae can be visualised by rotating the appendage using Drishti (see Figs. 9b, d; 17b). Another advantage of Drishti is the application of digital dissection and the removal of unwanted fragments (see Figs. 11a; 14; 15c).

The methodologies described here the combination of improved cleaning, digestion and preparation methods, allowing for reduced transfer of contaminants into the final slide mounts, the confocal data processing protocols and the possibility of post-acquisition removal of artefacts using free software have been shown to overcome all of the previous limitations in the use of confocal microscopy for the examination of small arthropods. Furthermore, the methodologies described for the use of Drishti to post-process samples have also been successfully applied to other confocal datasets and even been used for the production of 3D prints from the data.

The main limitation now remains the speed of the confocal microscope and its ability to handle and image larger specimens. “Macro confocal microscopes” have been assessed, but found to have inadequate resolution for this application. The use of high resolution micro-CT is currently being investigated as a complementary technique to provide further contextual 3D information on macro-invertebrates.

Acknowledgements

We acknowledge the two anonymous reviewers for their time, considerations and comments which improved this paper. We would like to thank Dr Tomasz Goral for their support obtaining images from the A1-Si confocal microscope and Dr Farah Ahmed, Dan Sykes and Rebecca Summerfield for assistance in training on Drishti (all staff in the Imaging and Analysis Centre, Natural History Museum, London). We also like to thank Dr Anthony J. Hayes and Dr Peter Watson (Bio imaging Unit, Cardiff School of Biosciences, Cardiff University) for making Zeiss LSM 880 airy scan upright confocal microscope available, Dr Christopher Wilkinson (School of Biological Science, Royal Holloway University of London) for providing access to the Olympus FV1000 IX81 inverted confocal microscope. This project was supported financially by the Republic of Turkey Ministry of National Education. Terue Kihara acknowledges funding from NHM departmental investment fund to run Confocal Microscopy workshop in February, 2015 at the Natural History Museum, London. Part of the project was supported by SYNTHESYS: DE-TAF-4692 for Paul Clark to study with Terue Kihara in the German Centre for Marine Biodiversity Research, Senckenberg am Meer, Wilhelmshaven.

References

Anger, K., Schreiber, D. & Montú, M. (1995) Abbreviated larval development of *Sesarma curacaoense* (Rathbun, 1897) (Decapoda: Grapsidae) reared in the laboratory. *Nauplius*. **3**, 127−154.

Bourke, P. (2011) Transferring slice data to Drishti using ImageJ. Retrieved from http://paulbourke.net/miscellaneous/Drishti_intro1/. Accessed 7 Oct 2016.

Böhm, A., Bartel, D., Szucsich, N.U. & Pass, G. (2011) Confocal imaging of the exo- and endoskeleton of Protura after non-destructive DNA extraction. *Soil Org.* **83**(3), 335−345.

Brandt, A., Brix, S., Held, C. & Kihara, T.C. (2014) Molecular differentiation in sympatry despite morphological stasis: deep-sea *Atlantoserolis* Wägele, 1994 and *Glabroserolis* Menzies, 1962 from the south-west Atlantic (Crustacea: Isopoda: Serolidae). *Zool. J. Linn. Soc.* **172**, 318−359. doi: 10.1111/zoj.12178

Brooker, A.J., Bron, J.E. & Shinn, A.P. (2012) Description of the free-swimming juvenile stages of *Lernaeocera branchialis* (Pennellidae), using traditional light and confocal microscopy. *Aquat. Biol*. **14**, 153−163. doi: 10.3354/ab00388

Brooker, A.J., Shinn, A.P. & Bron, J.E. (2012) Use of laser scanning confocal microscopy for morphological taxonomy and the potential for digital type specimens (e-types). *Aquat. Biol.* **14**, 165−173. doi: 10.3354/ab00389

Bundy M.H. & Paffenhöfer, G.A. (1993) Innervation of copepod antennules investigated using laser scanning confocal microscopy. *Mar. Ecol. Prog. Ser*. **102**, 1−14.

Butler, A.D., Edgecombe, G.D., Ball, A.D. & Giribet, G. (2010) Resolving the phylogenetic position of enigmatic New Guinea and Seychelles Scutigeromorpha (Chilopoda): a molecular and morphological assessment of Ballonemini. *Invertebr. Syst.* **24**, 539−559.

Buttino, I., Ianora, A., Carotenuto, Y., Zupo, V. & Miralto, A. (2003) Use of the confocal laser scanning microscope in studies on the developmental biology of marine crustaceans. *Microsc. Res. Tech*. **60**, 458−464.

Carotenuto, Y. (1999) Morphological analysis of larval stages of *Temora stylifera* (Copepoda, Calanoida) from the Mediterranean Sea. *J. Plankton. Res*. **21**(9), 1632−1632.

Clark, P.F. & Cuesta, J.A. (2015) Larval Systematics of Brachyura. *Decapoda: Brachyura, Treatise on Zoology – Anatomy, Taxonomy, Biology. The Crustacea, Complementary to the volumes translated from the French of the Trait´e de Zoologie [founded by P.-P. Grass´e (†)]*. (ed. by P. Castro, P.J.F. Davie, D. Guinot, F.R. Schram & J.C. Von Vaupel Klein), Chapter 71–17, 9(CII), pp. 981–1048. Brill, Leiden and Boston.

Coleman, C.O. (2006) Substituting time-consuming pencil drawings in arthropod taxonomy using stacks of digital photographs. *Zootaxa*. **1360**, 61–68.

Cuesta, J.A., Schuh, M., Diesel, R. & Schubart, C.D. (1999) Abbreviated development of *Armases miersii* (Grapsidae: Sesarminae), a crab that breeds in supralittoral rock pools. *J. Crust. Biol.* **19**(1), 26−41.

Dreszer, T.B., Raða, T. & Giribet, G. (2015) *Cyphophthalmus solentiensis* sp. nov. (Cyphophthalmi, Sironidae), a new endogean mite harvestman species from Croatia, with an application of confocal laser microscopy to illustrate genitalia in opiliones. *Bull. Mus. Comp. Zool*. **543**, 1−15. doi: http://dx.doi.org/10.3099/MCZ18.1

Felgenhauer, B.E. (1987) Techniques for preparing crustaceans for scanning electron microscopy. *J. Crust. Biol*. **7**, 71−76.

Fischer, C. & Ahlrichs, W.H. (2011) Revisiting the *Cephalodella trophi* types. *Hydrobiologia.* **662**(1), 205–209.

Galassi, D.M.P., Laurentiis, P.D. & Giammatteo, M. (1998) Integumental morphology in copepods: Assessment by confocal laser scanning microscopy (CLSM) (Crustacea, Copepoda). *Fragm. Entomol*. **30**(1), 79−92.

Kaji, T., Fritsch, M., Schwentner, M., Olesen, J. & Richter, S. (2014) Male claspers in clam shrimps (Crustacea, Branchiopoda) in the light of evolution: A case study on homology versus analogy. *J. Exp. Zool. (Mol. Dev. Evol.)*. **9999**, 1−12.

Kihara, T.C. & Martinez Arbizu, P. (2012) Three new species of *Cerviniella* Smirnov, 1946 (Copepoda: Harpacticoida) from the Arctic. *Zootaxa*. **3345**, 1−33.

Kihara, T.C. & Falavigna da Rocha, C.E. (2009) *Técnicas para estudo taxonomico de copepodes harpacticoides da meiofauna marinha*. Asterisco, Porto Alegre. pp. 96.

Kim, C.H. & Hwang S.G (1995) The complete larval development of the mitten crab *Eriocheir sinensis* H. Milne Edwards. 1853 (Decapoda, Brachyuran, Grapsidae) reared in the laboratory and a key to the known zoeae of the Varuninae. *Crustaceana*. **68**(7), 793−812.

Klaus, A.V., Kulasekera, V.L. & Schawaroch, V. (2003) Three-dimensional visualisation of insect morphology using confocal laser scanning microscopy. *J. Microsc*. **212**(2), 107−121.

Klaus, A.V. & Schawaroch, V. (2006) Novel methodology utilizing confocal laser scanning microscopy for systematic analysis in arthropods (Insecta). *Integr. Comp. Biol*. **46**(2), 207−214.

Lee, S., Brown, R.L. & Monroe, W. (2009) Use of confocal laser scanning microscopy in systematics of insects with a comparison of fluorescence from different stains. *Syst. Entomol*. **34**, 10−14.

Limaye, A. (2012) Drishti: a volume exploration and presentation tool. In *Proceedings of SPIE Vol. 8506 SPIE, Developments in X-Ray Tomography VIII Bellingham*, Stock, S.R. (ed.), WA. doi: 10.1117/12.935640.Lovett, B. (2013) The basics of Drishti. *Australian National*

University Internal Paper. 1–37. Retrieved from http://www.scribd.com/doc/191007517/The-Basics-of-Drishti-A-Free-To-Download-Volume-Exploration-Presentation-Tool.

Maruzzo, D., Minelli, A. & Fusco, G. (2009) Segmental mismatch in crustacean appendages: The naupliar antennal exopod of *Artemia* (Crustacea, Branchiopoda, Anostraca). *Arthropod. Struct. Dev*. **38**, 163–172.

Menzel, L. (2011) First descriptions of copepodid stages, sexual dimorphism and intraspecific variability of *Mesocletodes* Sars, 1909 (Copepoda, Harpacticoida, Argestidae), including the description of a new species with broad abyssal distribution. *ZooKeys*. **96**, 39–80. doi: 10.3897/zookeys.96.1496

McAllen, R. & Taylor, A. (2001) The effect of salinity change on the oxygen consumption and swimming activity of the high-shore rockpool copepod *Tigriopus brevicornis*. *J. Exp. Mar. Biol. Ecol*. **263**, 227−240.

Michels, J. (2007) Confocal laser scanning microscopy: using cuticular autofluorescence for high resolution morphological imaging in small crustaceans. *J. Microsc.* **227**(1), 1−7.

Michels, J. & Büntzow, M. (2010) Assessment of Congo red as a fluorescence marker for the exoskeleton of small crustaceans and the cuticle of polychaetes. *J. Microsc.* **238**(2), 95−101. doi: 10.1111/j.1365−2818.2009.03360

Michels, J. & Gorb, S.N. (2012) Detailed three-dimensional visualisation of resilin in the exoskeleton of arthropods using confocal laser scanning microscopy. *J. Microsc.* **245**(1), 1−16.

Michels, J., Vogt, J. & Gorb, S.N. (2012) Tools for crushing diatoms – opal teeth in copepods feature a rubber-like bearing composed of resilin. *Sci. Rep*. **2**, 465. doi: 10.1038/srep00465

Montu, M., Anger, K. & de Bakker, C. (1996) Larval development of the Chinese mitten crab *Eriocheir sinensis* H. Milne-Edwards (Decapoda: Grapsidae) reared in the laboratory. *Helgol. Meeresunters*. **50**, 223−252.

Schawaroch, V. & Li, S.C. (2007) Testing mounting media to eliminate background noise in confocal microscope 3-D images of insect genitalia. *Scanning*. **29**(4), 117–184.

Schneider, C.A., Rasband, W.S. & Eliceiri, K.W. (2012) NIH Image to ImageJ: 25 years of image analysis. *Nat. Methods*. **9**(7), 671−675.

Sewell, K.B. & Cannon, L.R.G. (1995) A scanning electron microscope study of *Craspedella* sp. from the branchial chamber of redclaw crayfish, *Cherax quadricarinatus*, from Queensland, Australia. *Hydrobiologia*. **305**, 151−158.

Valdecasas, A.G. (2008) Confocal microscopy applied to water mite taxonomy with the description of a new genus of Axonopsinae (Acari, Parasitengona, Hydrachnidia) from Central America. *Zootaxa*. **1820**, 41−48.

Valdecasas, A.G. & Abad, A. (2011) Morphological confocal microscopy in Arthropods and the enhancement of autofluorescence after proteinase K extraction. *Microsc. Microanal*. **17**, 109–113. doi: 10.1017/S1431927610094213

Wilkommen, J., Michels, J. & Gorb, S.N. (2015) Functional morphology of the male caudal appendages of the damselfly *Ischnura elegans* (Zygoptera: Coenagrionidae). *Arthropod. Struct. Dev*. **44**, 289−300.

Wolf, M. (2010) The reproductive ecology of a northeastern Pacific nudibranch, *Janolus fuscus*, with an examination of its endoparasitic copepod, *Ismaila belciki*. *Ph.D. Dissertation, University of Oregon, Eugene, Oregon*. Retrieved from https://scholarsbank.uoregon.edu/xmlui/handle/1794/11057.

Captions

Fig. 1. *Eriocheir sinensis*, zoea I, second maxilliped. A comparison of (a) SEM image obtained using Zeiss Ultra Plus Field Emission. (b) Line drawing from Kim & Hwang (1995). (c) Line drawing from Montu *et al*. (1996). (d) Drishti image obtained using Nikon A1-Si CLSM. Scale bars a = 20 μm; b-d = 100 μm.

Fig. 2. A flowchart for visualisation and 3D imaging of brachyuran crab larvae.

Fig. 3. *Eriocheir sinensis* zoeal stages using Nikon A1-Si CLSM. Confocal images. (a) ZI, 10× dry objective. (b) ZII, 10× dry objective applying "large images" option, scan area of 2×1 fields for image stitching. (c) ZIII, 10× dry objective applying "large images" option, scan area of 2×2 fields for image stitching. (d) ZIV, 10× dry objective applying "large images" option, scan area of 3×2 fields for image stitching. (e) ZV, 10× dry objective applying "large images" option, scan area of 4×3 fields for image stitching. (f) ZVI, 10× dry objective applying "large images" option, scan area of 4×4 fields for image stitching. Scale bars = 500 μm.

Fig. 4. Preparation of slide using reinforcement rings.

Fig. 5. *Eriocheir sinensis*, zoea II, Drishti images of first maxilliped using Nikon A1-Si CLSM. (a) Basis and endopod, scan area of 1×2 fields for image stitching, 20× dry immersion objective applying "large images" option. (b) Endopod. (c) Basis. Both using 40× oil immersion objective. (d) Basis and endopod merged from two images using Adobe Photoshop, after applying ImageJ and Drishti. Scale bars a = 300 μm; b-d = 100 μm.

Fig. 6. File formats of different confocal microscopes. Leica uses ***.lif files. Nikon uses ***.nd2 files. Olympus uses ***.oib files. Zeiss uses ***.czi files.

Fig. 7. *Eriocheir sinensis*, zoeae with debris adhered to the exoskeleton. (a) ZI showing calcium carbonate using SEM LEO 1455 VP analysis. (b) ZII, confocal image of endopod using Nikon A1-Si CLSM, 60× oil immersion objective. (c) ZII, Drishti image of endopod. (d) ZII, attempt

at debris removal using Drishti and Photoshop was not always successful, see circled areas. Scale bars a = 300 μm; b-d= 100 μm.

Fig. 8. Advantages of staining and digesting appendages. *Eriocheir sinensis*, zoea I, scanned images of the maxilla using Nikon A1-Si CLSM. (a) Undigested and unstained, 60× oil immersion objective. (b) Digested and stained with Congo red and acid fuchsin, 40× oil immersion objective. (c) Undigested and stained using only Congo red, 60× oil immersion objective. (d) Undigested and stained using the mixture of Congo red and acid fuchsin, 40× oil immersion objectives. Scale bars a, c = 50 μm; b, d = 100 μm.

Fig. 9. Advantages of digesting appendages. *Eriocheir sinensis*, zoea I, images of second maxilliped using Nikon A1-Si CLSM. (a) Confocal image of non-digested appendage showing basial musculature. (b) Drishti image of non-digested appendage. c) Confocal image of digested basial muscles. (d) Drishti image of digested appendage (tiny structures are circled). All 40× oil immersion objective, applying "large images" option, scan area of 1×2 fields for image stitching. Scale bars = 100 μm.

Fig. 10. "Tiling" appendages when scanning at higher magnification. *Eriocheir sinensis*, zoea V, image of maxilla using Nikon A1-Si CLSM. (a) Confocal image showing tiled areas. (b) Drishti image. 40× oil immersion objective, applying "large images" option, scan area of 2×3 fields for image stitching. Scale bars a = 100 μm; b = 200 μm.

Fig. 11. Merging Drishti images using Adobe Photoshop. *Eriocheir sinensis* zoeal appendages using Nikon A1-Si CLSM. (a) ZII, maxilla, 40× oil immersion objective. (b) ZI, lateral view of pleon, 20× dry immersion objective. Scale bars a = 200 μm; b = 300 μm.

Fig. 12. Visualisation of fine setae. *Eriocheir sinensis*, zoea I. Image of dorsal view of pleon using Nikon A1-Si CLSM, 40× oil immersion objective, applying "large images" option, scan area of 2×6 fields for image stitching. Scale bar = 200 μm.

Fig. 13. Scanned brachyuran crab larvae using different brands of CLSM processed in Drishti. *Eriocheir sinensis*, zoea I, first maxilliped. (a) Basis, Nikon A1-Si CLSM. (b) Endopod, Olympus Fluoview FV1000 IX8. (c) Antenna, Zeiss LSM 880 airy scan. All 40× oil immersion objective. (d) *Sesarma curacaoense*, ZIV, lateral view of pleon, Leica TCS SP5, 10× dry objective. Scale bars a-b = 100 μm; c = 50 μm; d =500 μm.

Fig. 14. Digital dissection. *Eriocheir sinensis*, zoea I, image of maxillule using Nikon A1-Si CLSM and processed using Drishti. (a) Unwanted tissue arrowed. (b) Repositioning of appendage to allow the removal of unwanted tissue (arrowed). (c) After digital dissection of tissue (compare a with c). 40× oil immersion objective. Scale bars = 100 μm.

Fig. 15. Drishti images of *Eriocheir sinensis* zoeal appendages using Nikon A1-Si CLSM: (a) ZII, antennule, 40× oil immersion objective. (b) ZI, antenna, 60× oil immersion objective. (c) ZI, maxillule, 40× oil immersion objective. Scale bars a, c = 100 μm; b = 50 μm.

Fig. 16. Drishti images of *Sesarma curacaoense*, zoea I appendages using Leica TCS SP5. First maxilliped. (a) Coxa and basis. (b) Endopod. (c) Coxa and basis of second maxilliped. (d) Maxillule. All 40× oil immersion objective. Scale bars a-b = 50 μm; c-d = 100 μm.

Fig. 17. Drishti images of *Armases miersii*, zoea IV appendages using Leica TCS SP5. (a) Coxa and basis of first maxilliped. (b) Endopod of second maxilliped. Both using 40× oil immersion objective. (c) Antenna. (d) Maxillule. Both using 20× dry objective. Scale bars a, d = 200 μm; b-c = 100 μm.

Fig. 18. Comparing bright field and confocal images. *Eriocheir sinensis* zoea, images of second maxilliped using Nikon A1-Si CLSM. (a) ZI, bright field image of exopod, 20× dry objective. (b) ZIV, confocal image of exopod, 20× dry objective applying "large images" option, scan area of 1×2 fields for image stitching. Scale bars a = 50 μm; b = 100 μm.

Supporting Information

1. SEM preparation

Laboratory hatched first stage zoeae of Chinese mitten crabs (*Eriocheir sinensis*), previously fixed in 70% ethanol and deposited in the crustacean reference collections of the NHM, were used for SEM examination. Zoea I larvae contaminated with debris were cleaned using Decon 90. Two or three drops of Decon 90 were added to 100 ml of 70% ethanol and specimens were left in this solution for 3 to 4 hours. This solution was occasionally gently agitated by hand. The sonication step as proposed by Felgenhauer (1987) or use of a tumbler were ignored as it often resulted in natatory setae of the maxillipeds becoming tangled. After cleaning, the specimens were pipetted into deionised water for 5 minutes and washed thoroughly including three changes of 5 minutes each. Next, the specimens were transferred to 30% ethanol from distilled water as the first step of the dehydration process. This was left for 30 minutes and later refilled with 30% ethanol for another 30 minutes. Then this step was applied to each concentration of the following until 100% dried ethanol.

50% ethanol (2 × 30 min)

70% ethanol (2 × 30 min)

80% ethanol (2 × 30 min)

90% ethanol (2 × 30 min)

95% ethanol (2 × 30 min)

100% dried ethanol (2 × 30 min)

The specimens were then critical point dried prior to mounting and coating for SEM observation using a Zeiss Ultra Plus Field Emission SEM (see Fig. 1a). For debris analysis, samples were examined, uncoated, using a LEO 1455 VP SEM (see Fig, 7a).

2. Preparation of SDS +DTT solution

Stock solution of SDS was prepared by adding 5.2 g (0.18 M) SDS (sodium dodecyl sulphate) and 0.24 g (0.03 M) NH_4HCO_3 (ammonium hydrogen carbonate) to 100 ml deionised water in an Erlenmeyer flask (pH 8.3). Then, the reducing agent, 0.1 g DTT (1,4-dithio-DL-threitol) was added to a 5 ml stock solution of SDS in a glass vial using a micropipette before each digestion process. The mixture of SDS + DTT was then shaken vigorously. The stock solution of SDS can be safely stored in a fridge for up to 6 months. Once SDS is mixed with DTT, the mixture should be used within a week as the mixture should be fresh.

3. Exporting stack data into ImageJ

Any stack data file can be opened in ImageJ. Opening ImageJ software programme (Supp. Fig. 1), go to File> Open> click on data; click open (Supp. Fig. 2).

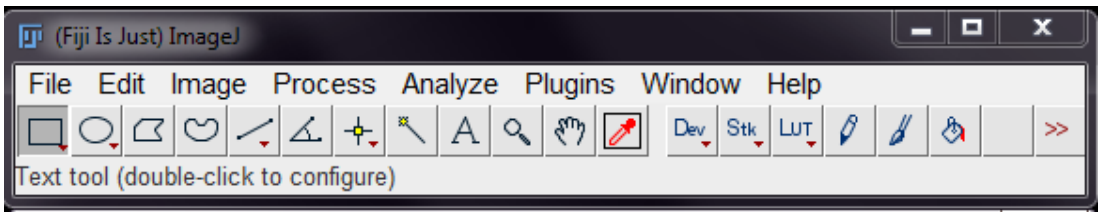

Supp. Fig. 1. The menu bar for ImageJ.

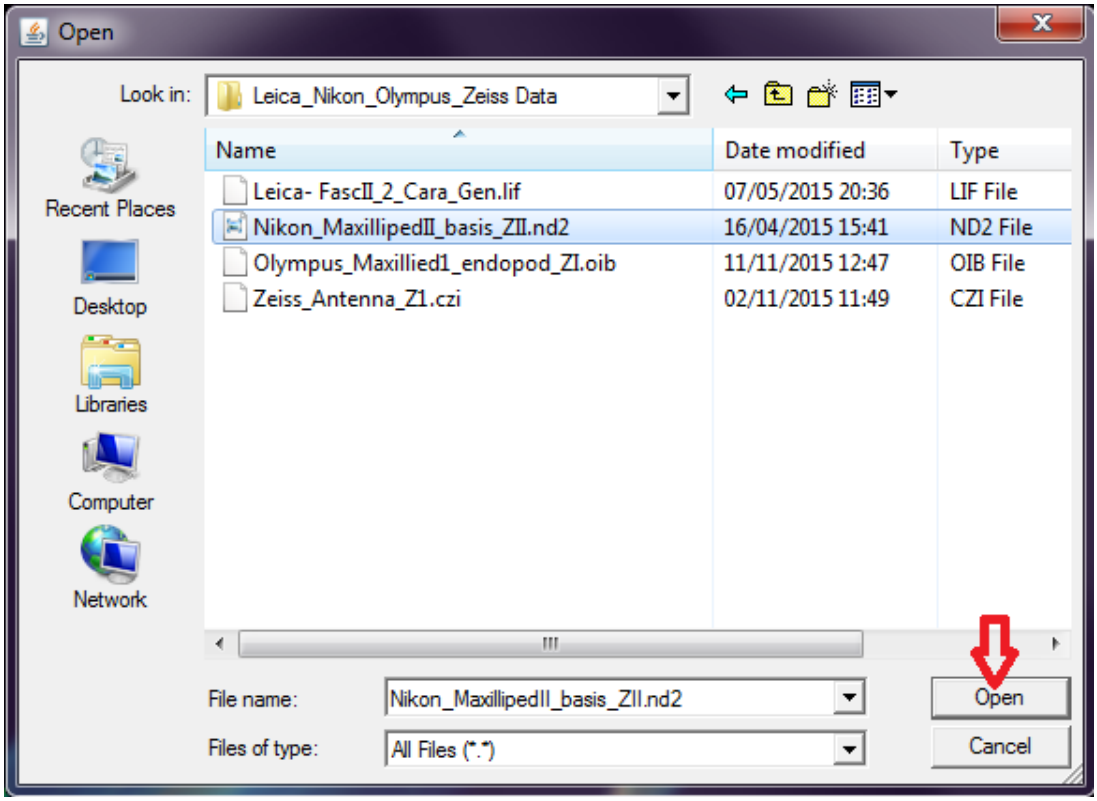

Supp. Fig. 2. Opening stack data in ImageJ, e.g. Nikon_MaxillipedII_basis_ZII.nd2 has been selected.

Open stack data; select “Grayscale” from dropdown menu and select options “Autoscale” and “Split channels”; click OK (Supp. Fig. 3).

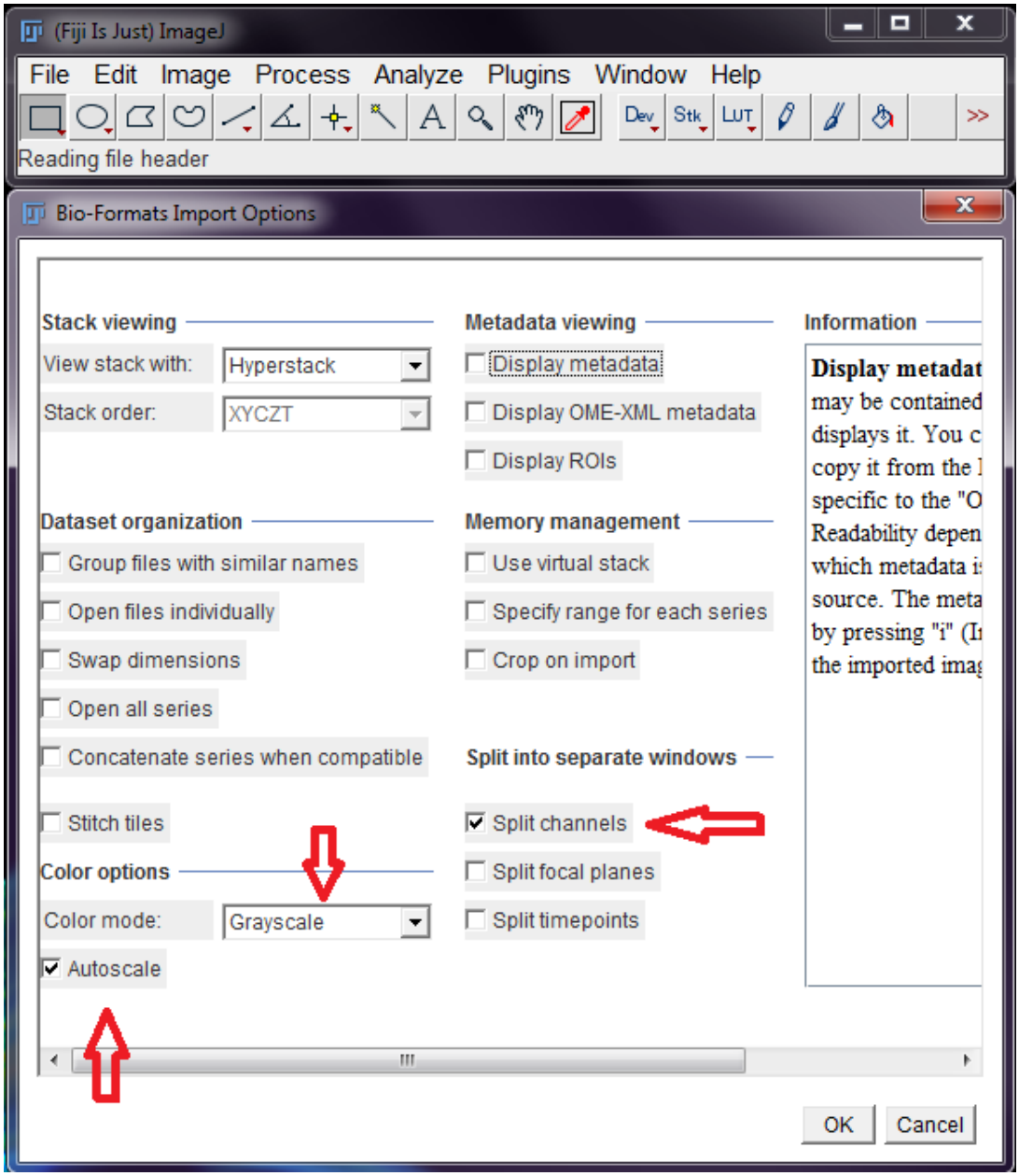

Supp. Fig. 3. Import options for stack data.

The stack data will split into the number of channels scanned, in this example 4 (see Supp. Fig. 4); go to Image> Properties; note image properties (voxel size), this information is required for the reconstruction of an accurate scale bar in the final images. In this example, pixel width represents X, pixel height represents Y and voxel depth represents Z in microns. Record image properties, e.g. x = 0.31, y = 0.31 and z = 0.7 microns; click OK (Supp. Fig. 4).

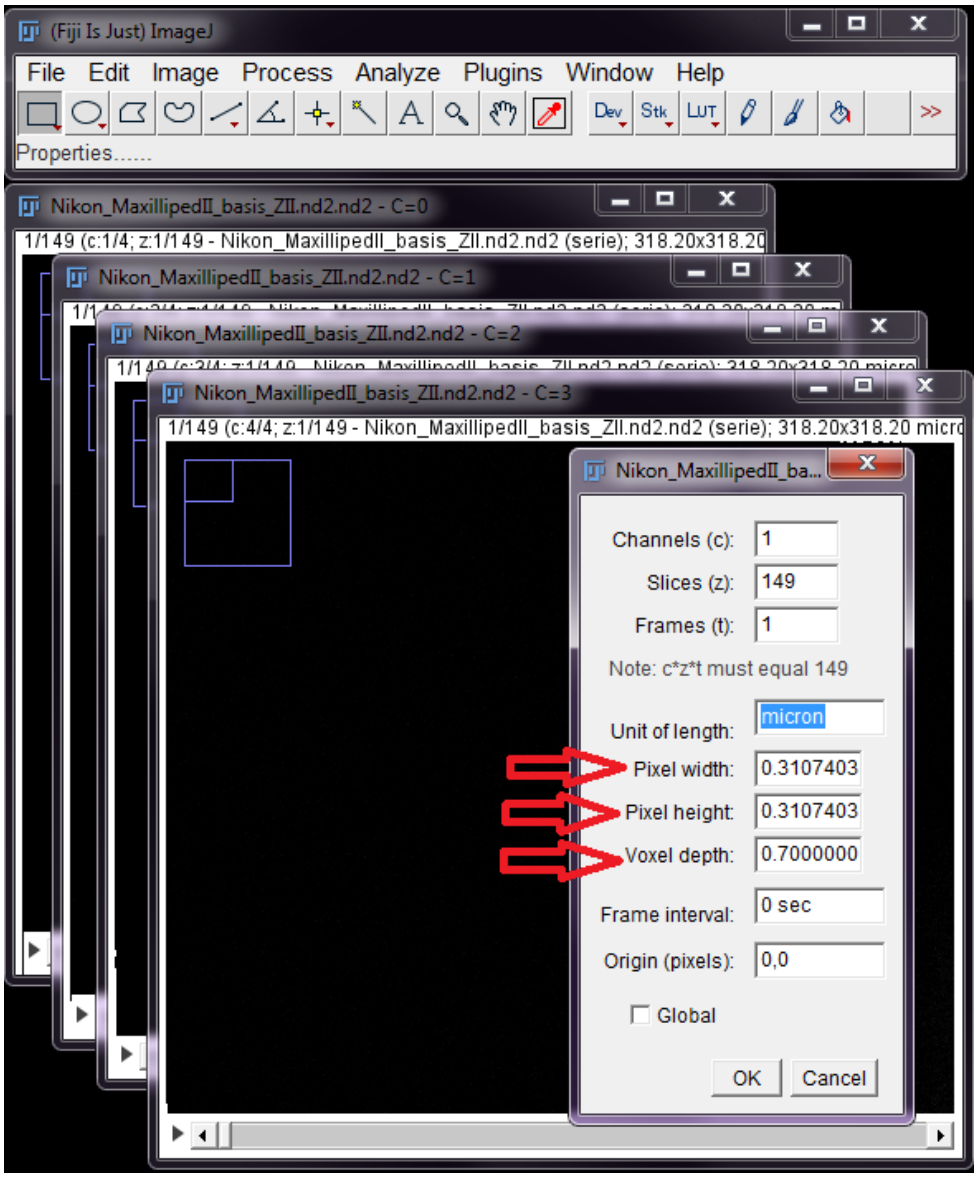

Supp. Fig. 4. Record image properties (voxel size) for later use, e.g. x = 0.31, y = 0.31 and z = 0.7 microns.

Now check scanned image quality of each channel: click ► to play image stacks; any channel not providing full information, e.g. corrupted scans, oversaturated images, or high level of background noise, these channels should not be selected when merging channels (Supp. Fig. 5).

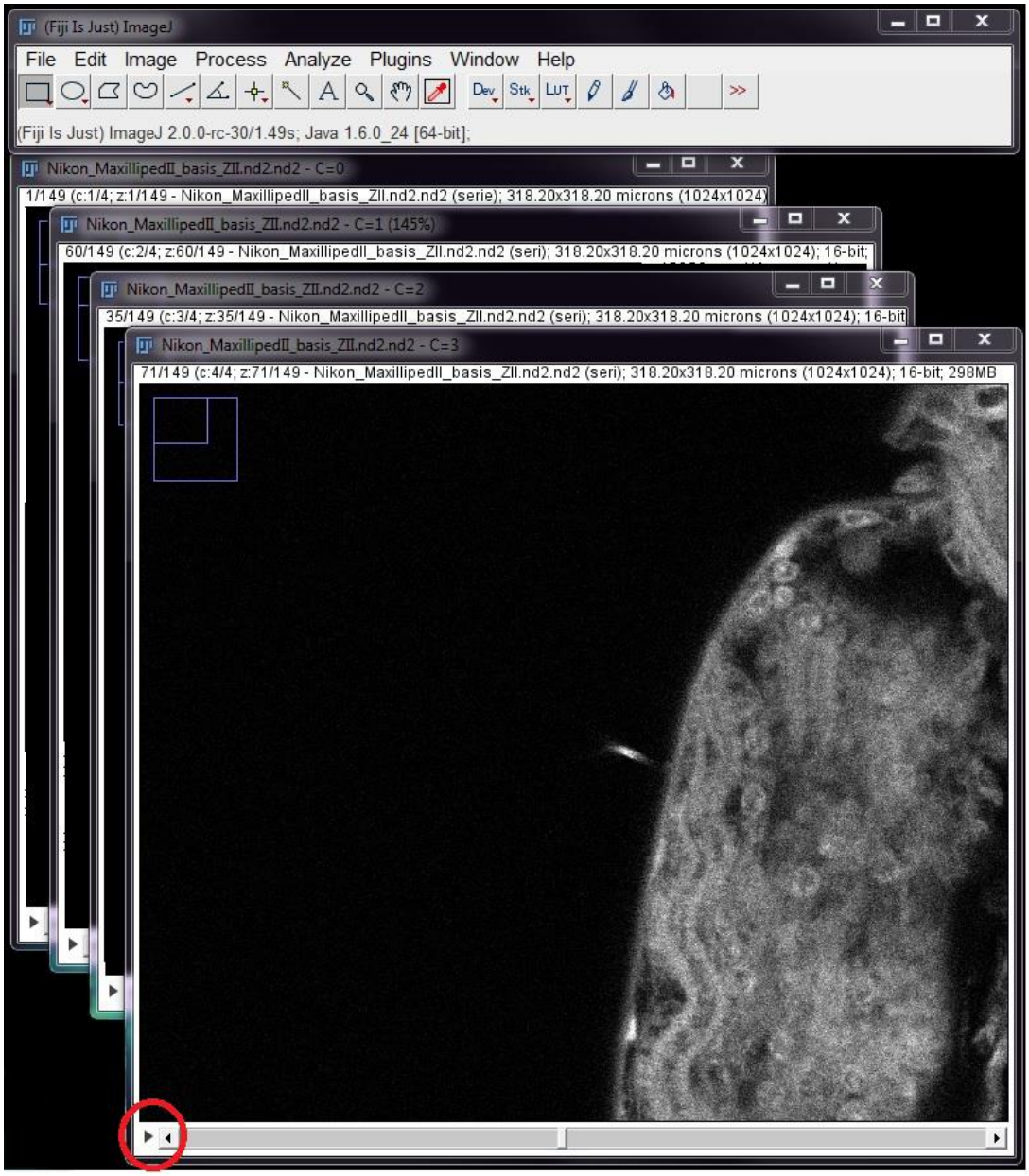

Supp. Fig. 5. Click on ► to check image quality for each channel.

Go to Image> Color> Merge Channels… and click (Supp. Fig. 6).

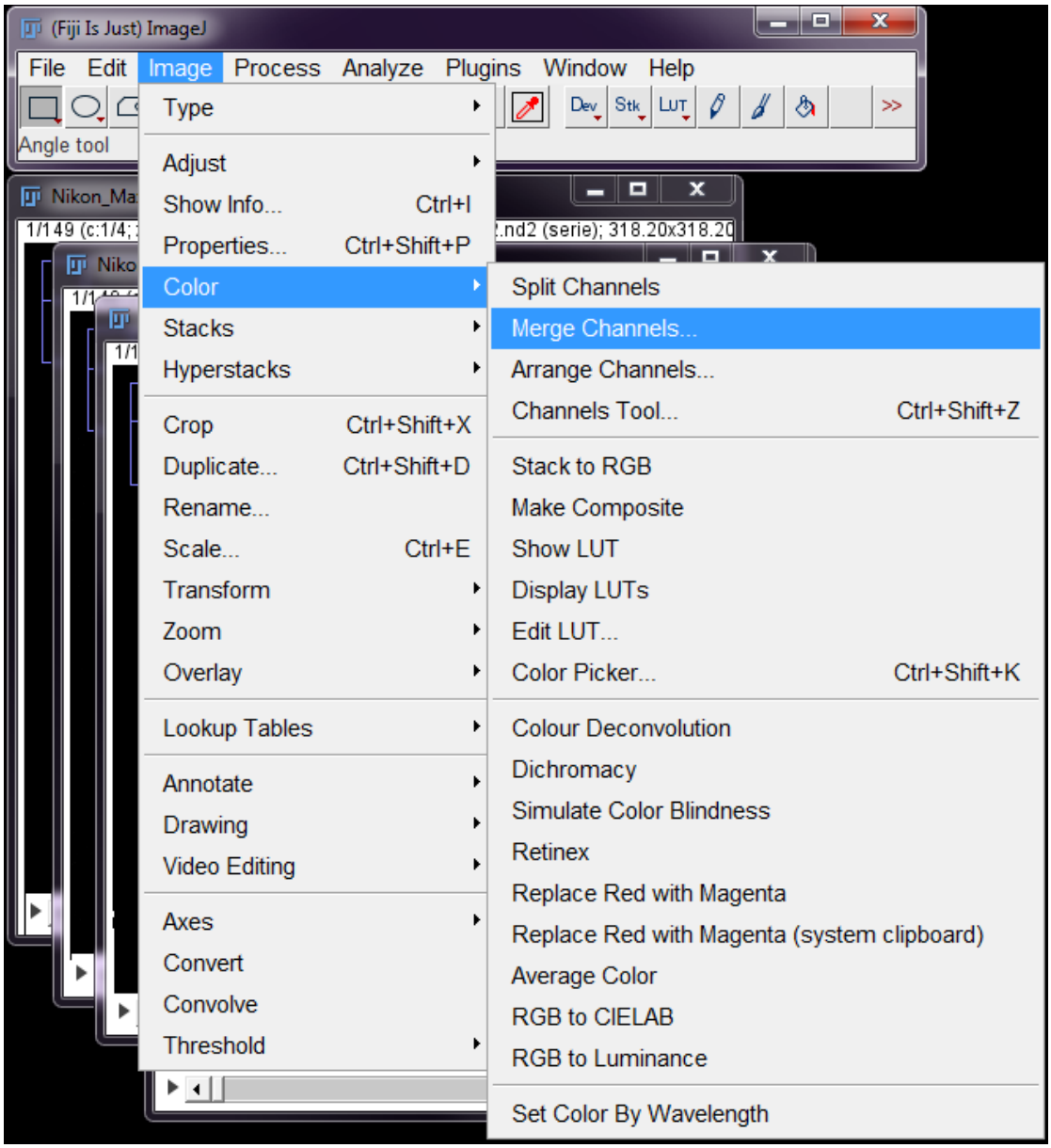

Supp. Fig. 6. Merging selected channels in ImageJ.

Select channels to be merged by clicking ▼; any channels not selected due to poor quality will not be merged; after selecting channels, click option “Create composite”; click OK (Supp. Fig. 7).

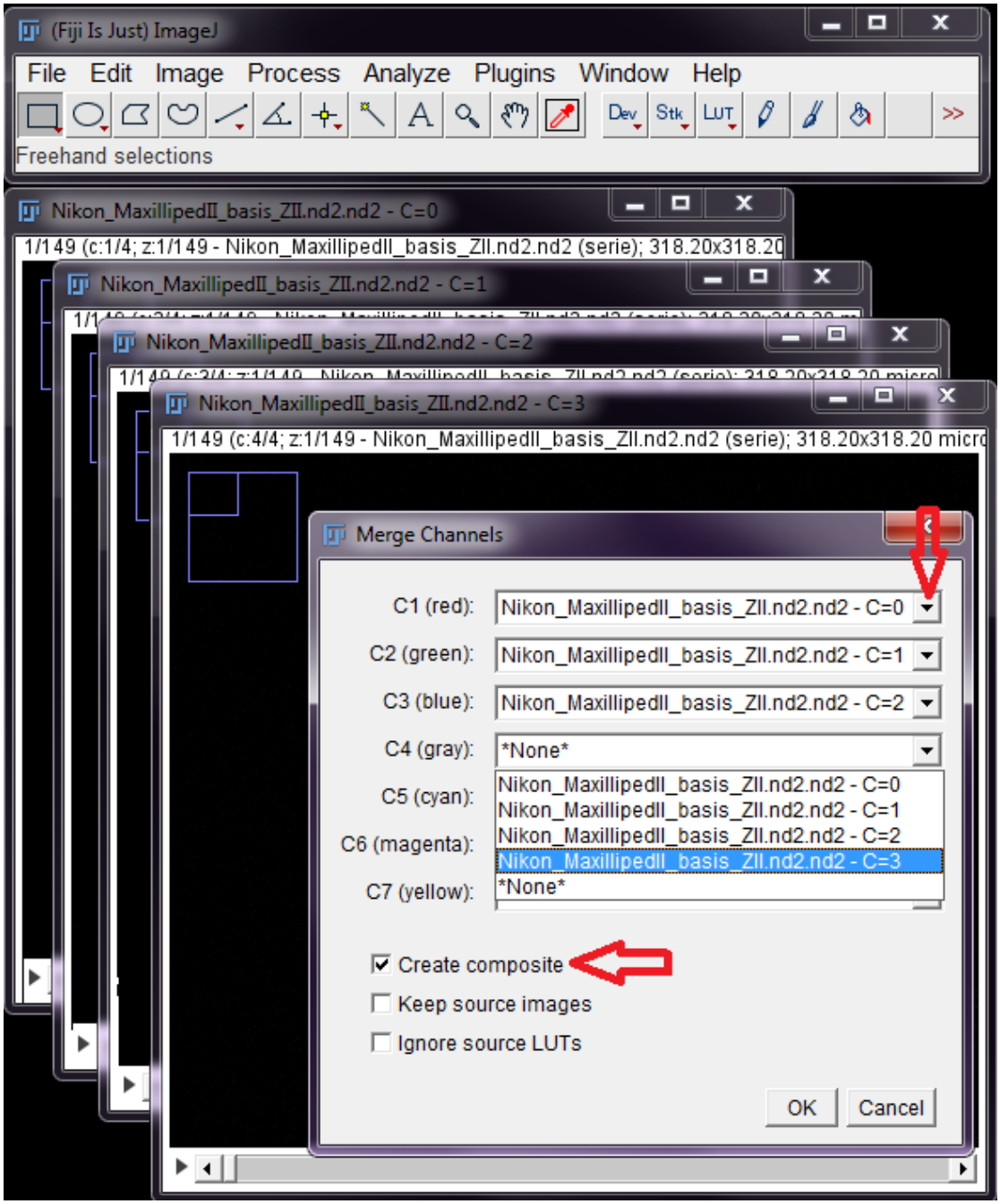

Supp. Fig. 7. Selecting channels to be merged.

Next, go to Image> Color> Channels Tool…, click; More> Convert to RGB, click OK (Supp. Figs. 8−10).

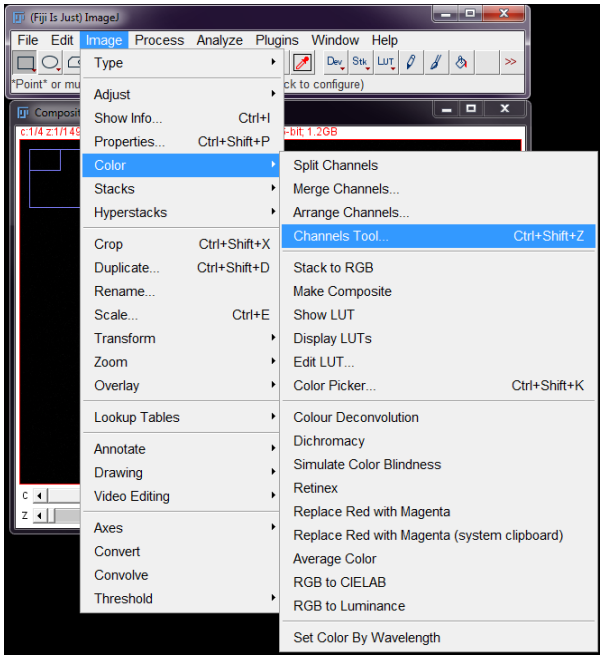

Supp. Fig. 8. Go to Image> Color> Channels Tool….

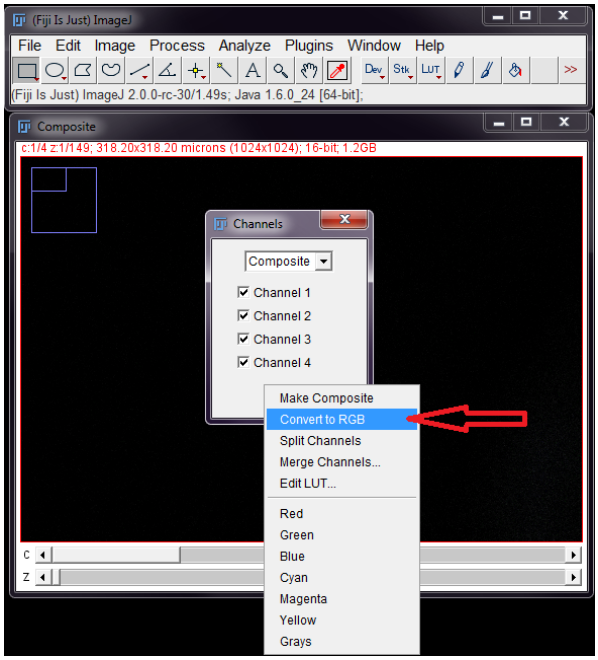

Supp. Fig. 9. Convert to RGB.

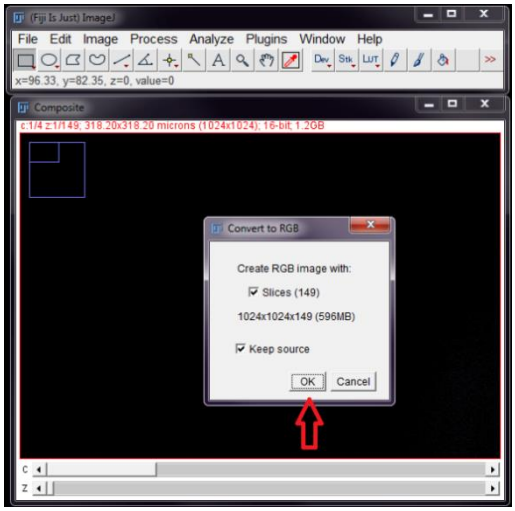

Supp. Fig. 10. Following ImageJ instructions.

Next converted single merged channel from RGB color to 8-bit image; go to Image> Type and click 8-bit (Supp. Fig. 11).

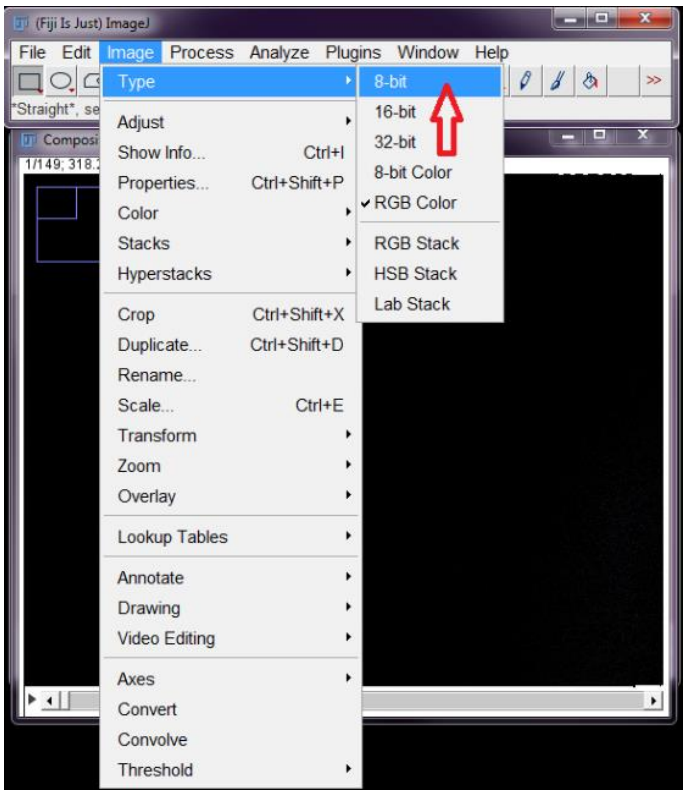

Supp. Fig. 11. Changing image from RGB color to 8-bit in ImageJ.

Then go to File> Save as > Image Sequence… and click; then OK in TIFF format (Supp. Figs. 12−13).

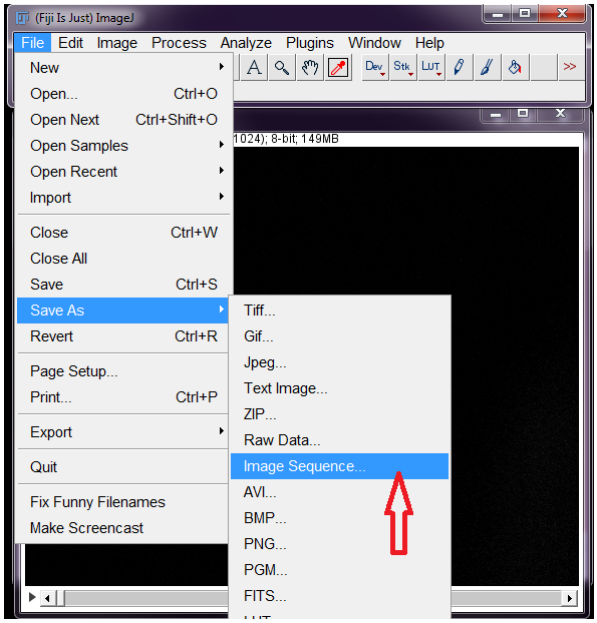

Supp. Fig. 12. Save merged channel image stacks as image sequence.

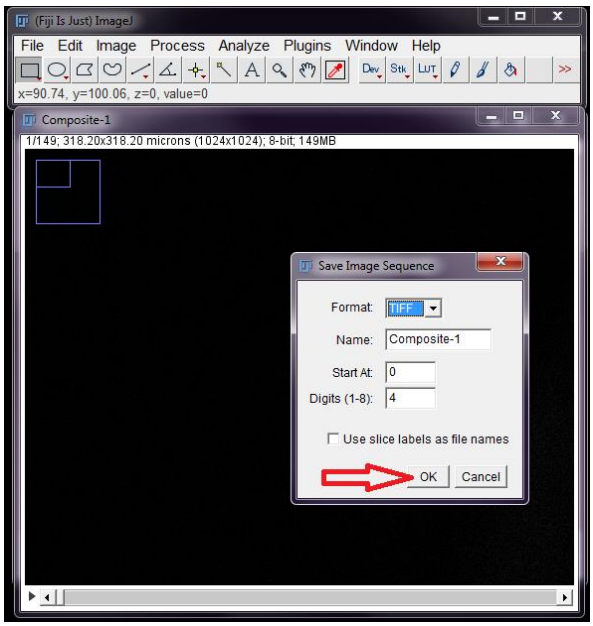

Supp. Fig. 13. Save merged channel image stacks to TIFF format; click OK.

Create and name a new folder; save image stacks to folder; click save (Supp. Fig. 14).

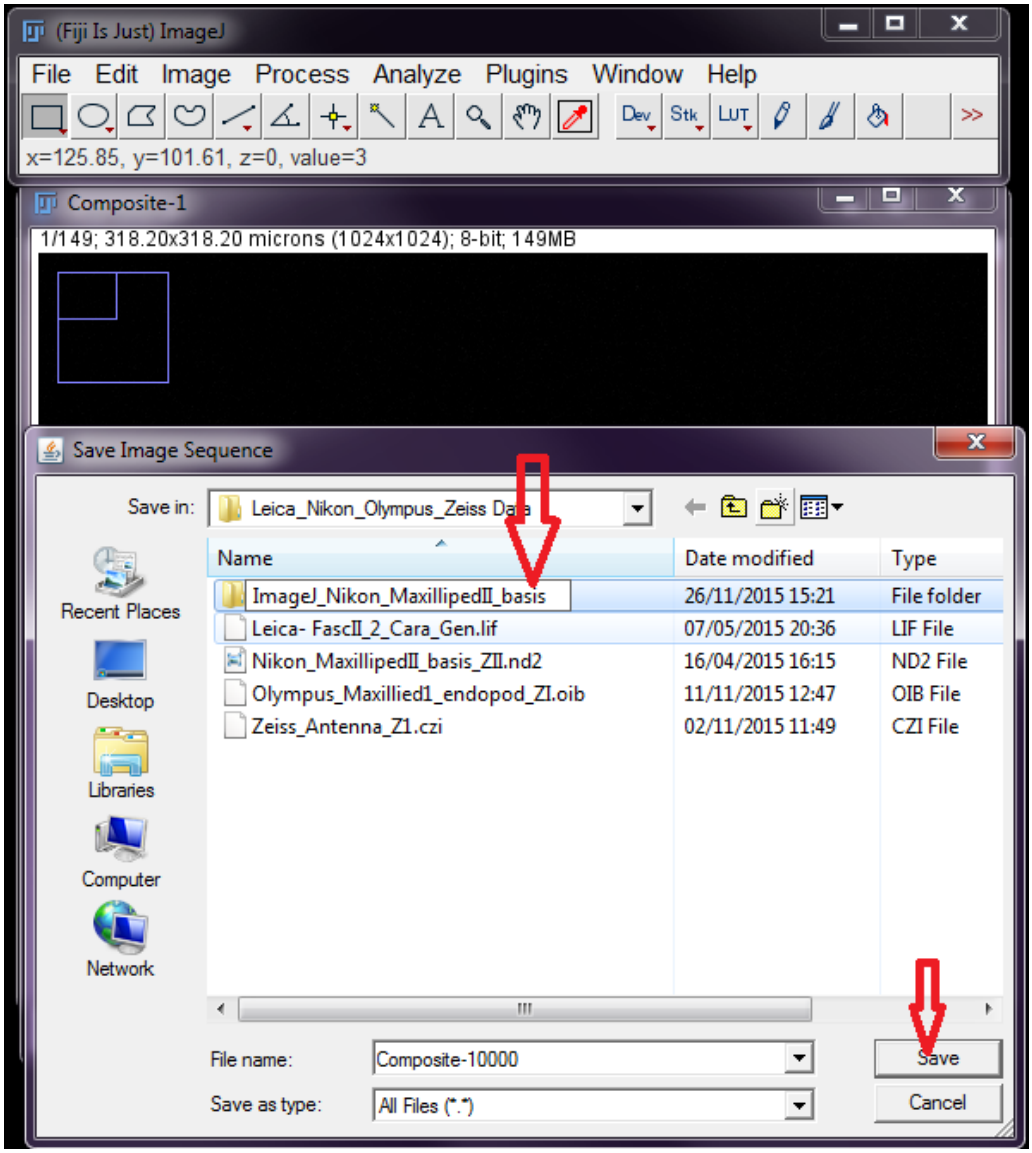

Supp. Fig. 14. Save merged image stacks to new folder, e.g. ImageJ_Nikon_Maxilliped II_basis.

4. Importing stack data into Drishtiimport

Go to http://sf.anu.edu.au/Vizlab/drishti/ and download Drishti. After downloading use "drishtiimport - Shortcut" icon (Supp. Fig. 15).

Supp. Fig. 15. Shortcut icon for "drishtiimport".

Click on "drishti - Shortcut" icon and a blank window will appear. From post-processing (3D Modelling) treatment, drag and drop either a new folder from the standard option (e.g. "Orange channel") or ImageJ (e.g. "ImageJ_Nikon_Maxilliped II_basis") into the "drishtiimport" window and the "Select Directory Type" window will automatically open; select 6th option "Grayscale TIFF Image Directory" (Supp. Fig. 16).

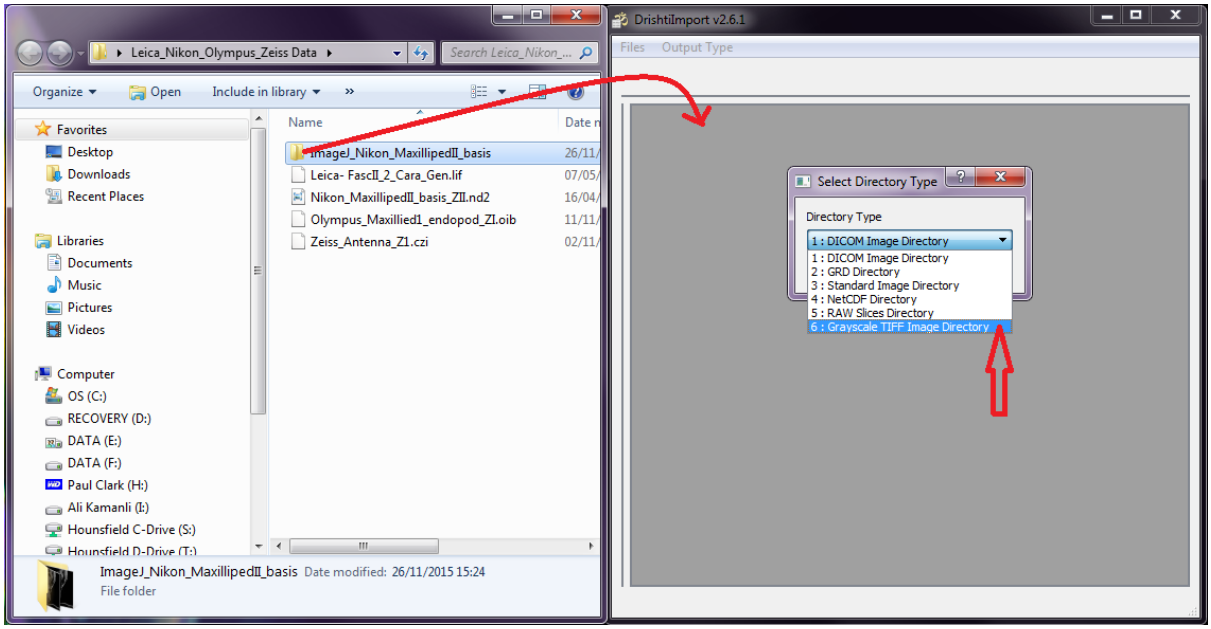

Supp. Fig. 16. Importing post-processing data into Drishtiimport.

"Select Voxel Type" window appears; click OK (Supp. Fig. 17).

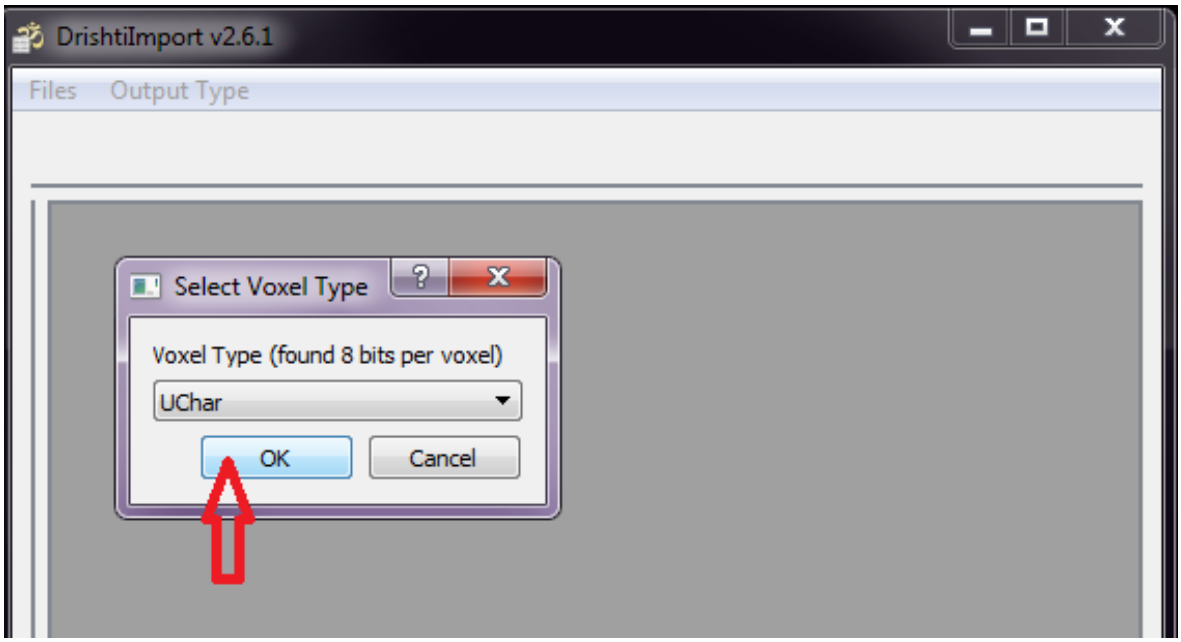

Supp. Fig. 17. Following instruction for importing the data to Drishti.

Go to File> Save as (S) and name new file ***.pvl.nc which are referred to as volumes in Drishti, e.g. “MaxillipedII_basis_Drishti_import.pvl.nc”; click save (Supp. Fig. 18).

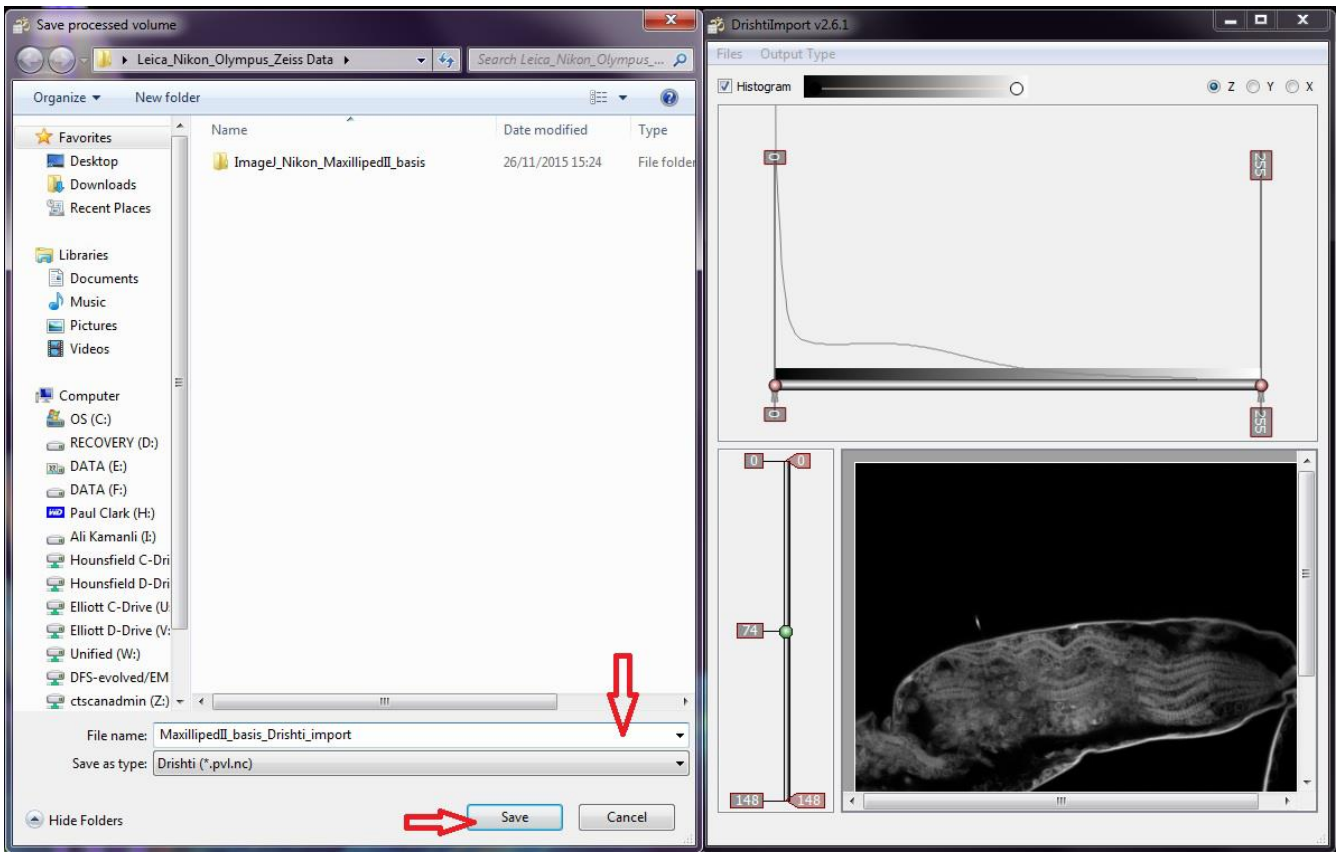

Supp. Fig. 18. Save to ***.pvl.nc file which are referred to as volumes in Drishti.

A series of 5 windows will appear respectively; click OK (Supp. Fig. 19a-e).

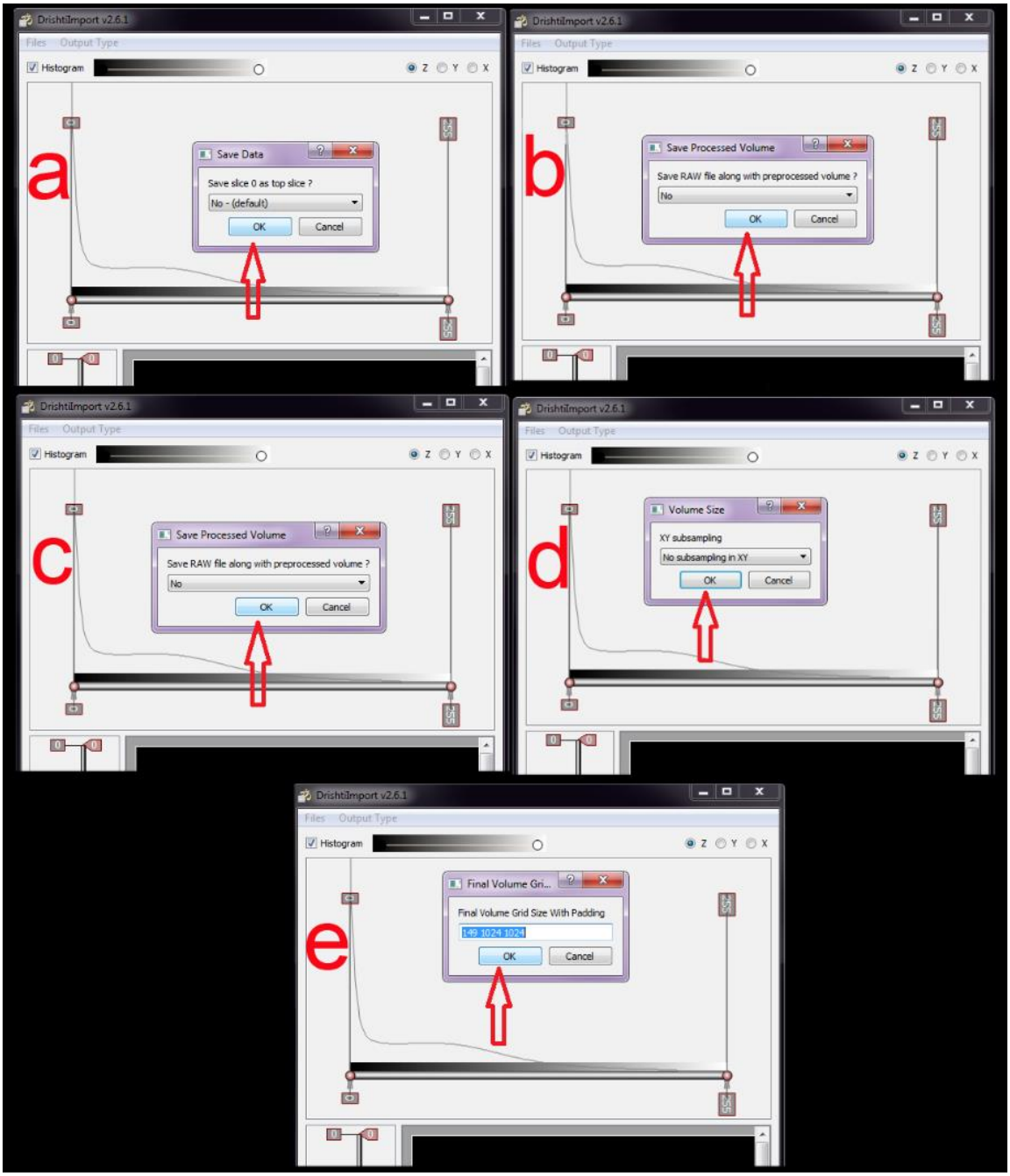

Supp. Fig. 19. Following save, a series of 5 windows will open; for each click OK.

The “Additional Information” window appears; recover noted “image properties” (voxel size) recorded from the standard manufacturers package or ImageJ (Supp. Fig. 4) and enter data manually by leaving one-character space between, x, y, and z values e.g. 0.31 nm, 0.31 nm and 0.7 nm; click OK (Supp. Fig. 20).

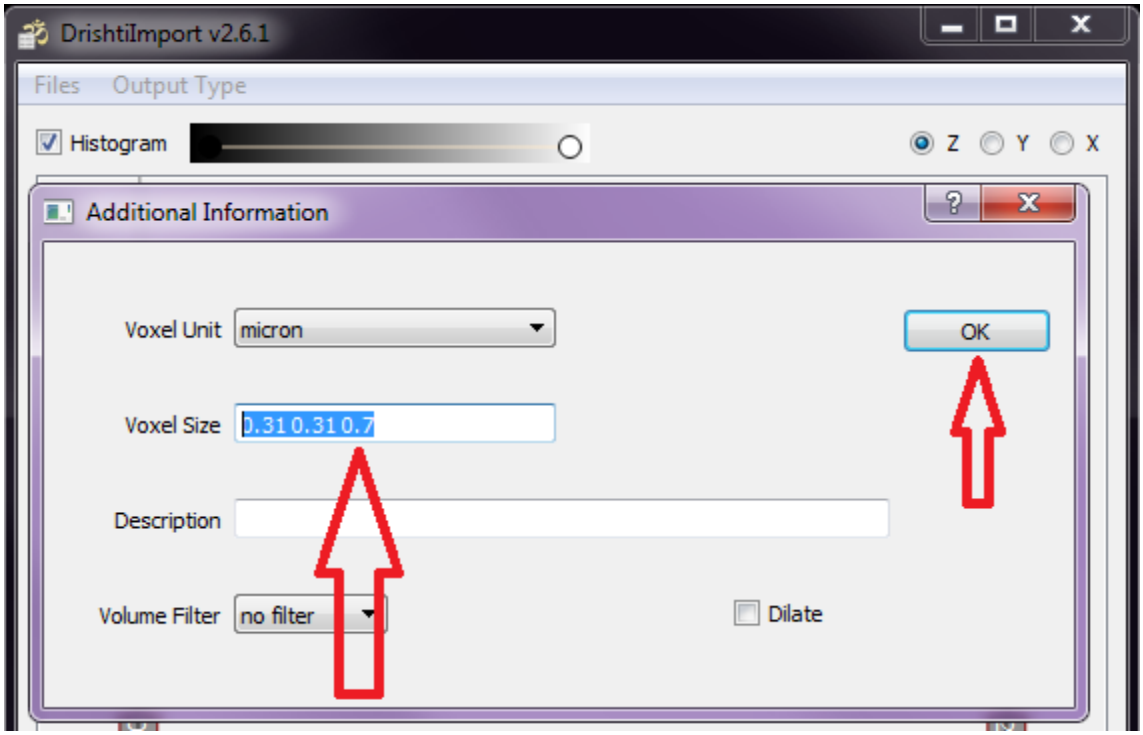

Supp. Fig. 20. Entering “image properties” (voxel size); x, y and z values.

Click OK when “Done” appears. File will be saved as “MaxillipedII_basis_Drishti_import.pvl.nc”and“MaxillipedII_basis_Drishti_import.pvl.nc001” (Supp. Fig. 21).

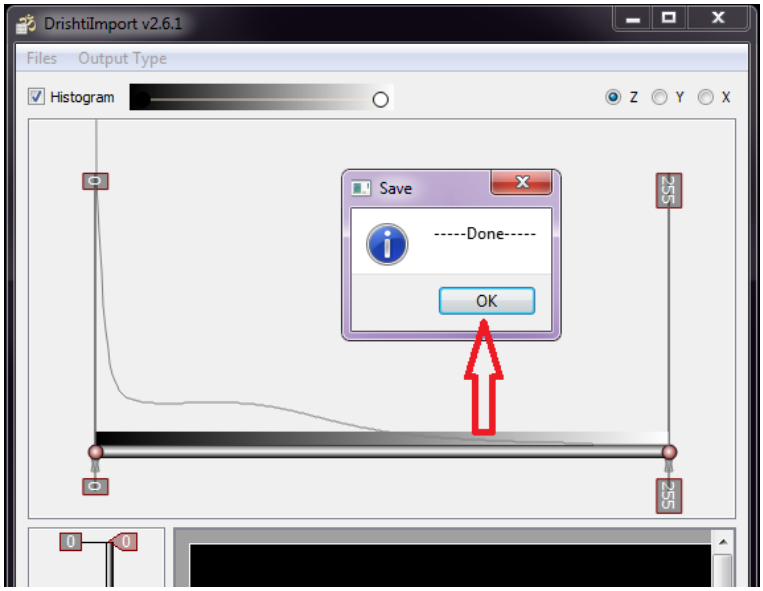

Supp. Fig. 21. Saving the data to use in Drishti.

5. Drishti visualisation instructions

Open "Drishti" (Supp. Fig. 22); and either drag and drop the ***.pvl.nc file from drishtiimport or go to File> Load volume> Load one volume and select the ***.pvl.nc file, e.g. "MaxillipedII_basis_Drishti_import.pvl.nc" (Supp. Fig. 23).

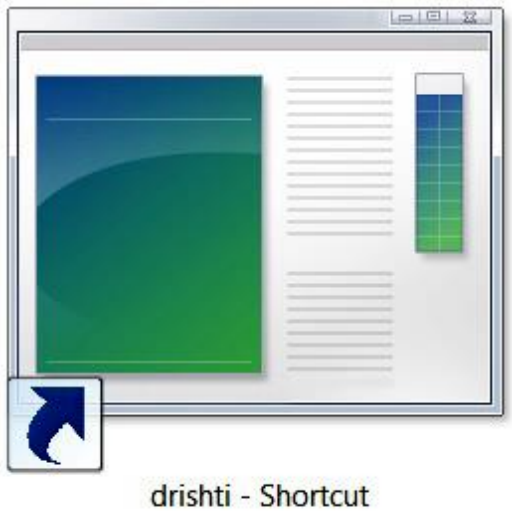

Supp. Fig. 22. Shortcut icon for "Drishti".

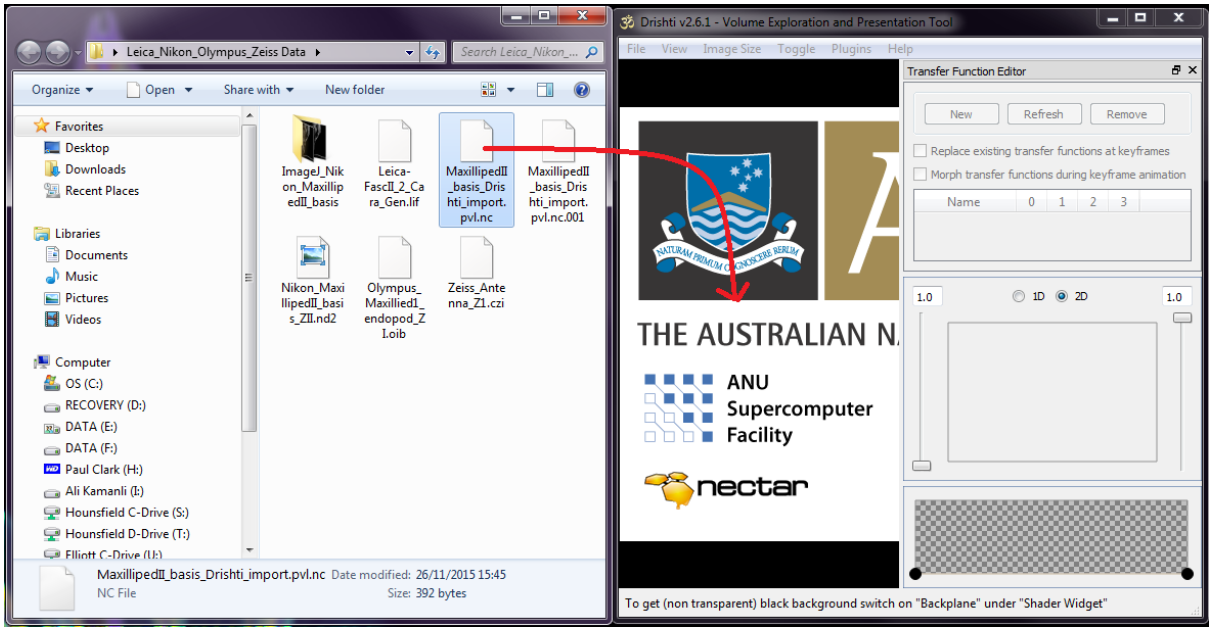

Supp. Fig. 23. Load ***.pvl.nc file, e.g. “MaxillipedII_basis_Drishti_import.pvl.nc” into Drishti.

A 3D representation of the file can now be viewed. This initial volume can be cropped to fit the scanned image; left click and drag the crossed square when the red line appears (Supp. Fig. 24).

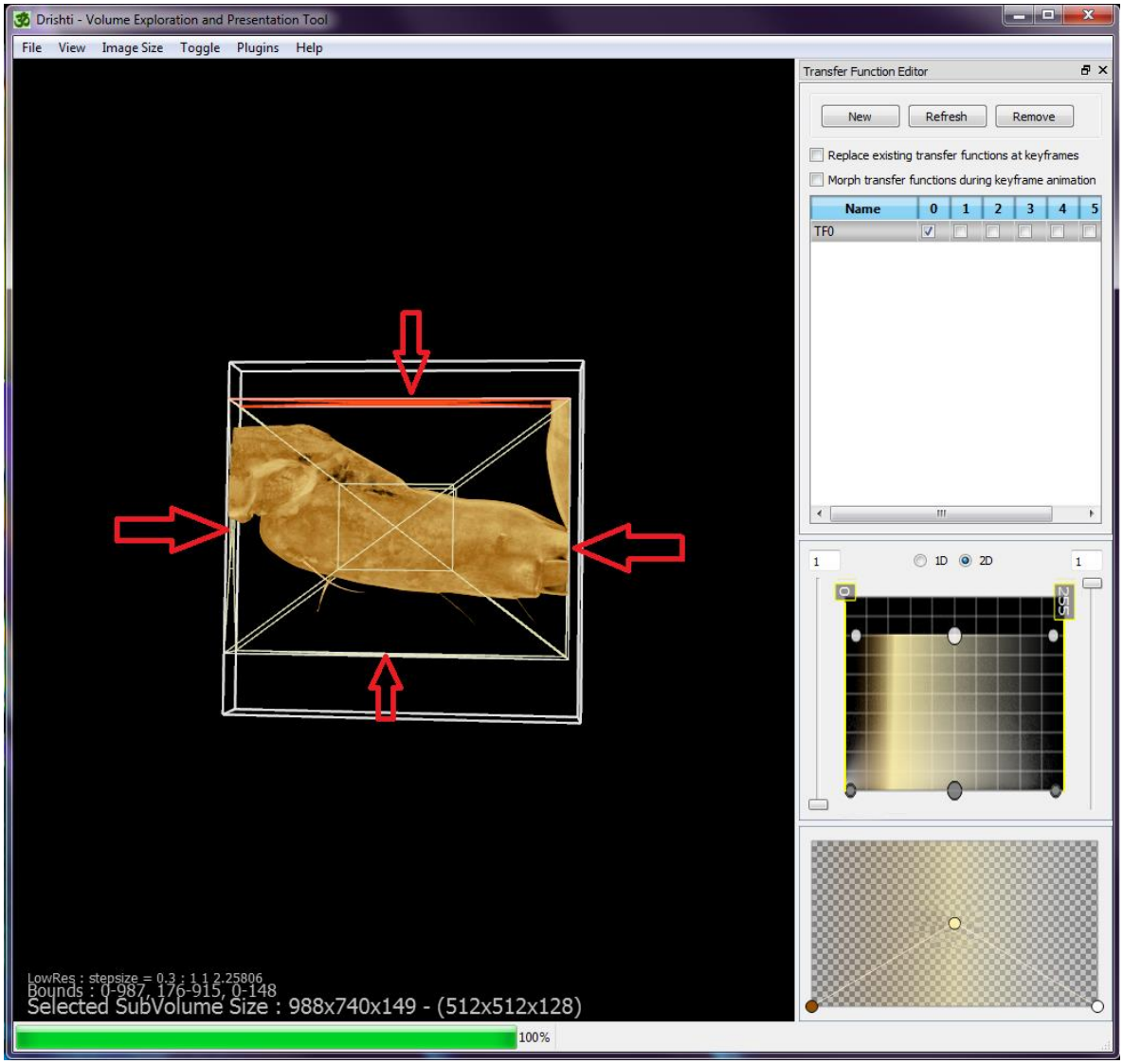

Supp. Fig. 24. Cropping the initial scanned volume.

F2 is used to toggle between high resolution and standard mode. 1 is used to toggle the lighting. B is used to toggle between box frames present or absent. To zoom in/out the mouse wheel is used. Image quality and background colour can be adjusted, go to View> Preferences (see arrows on left of main window). For adjustments of offset and intensity of image use buttons in right window (Supp. Fig. 25).

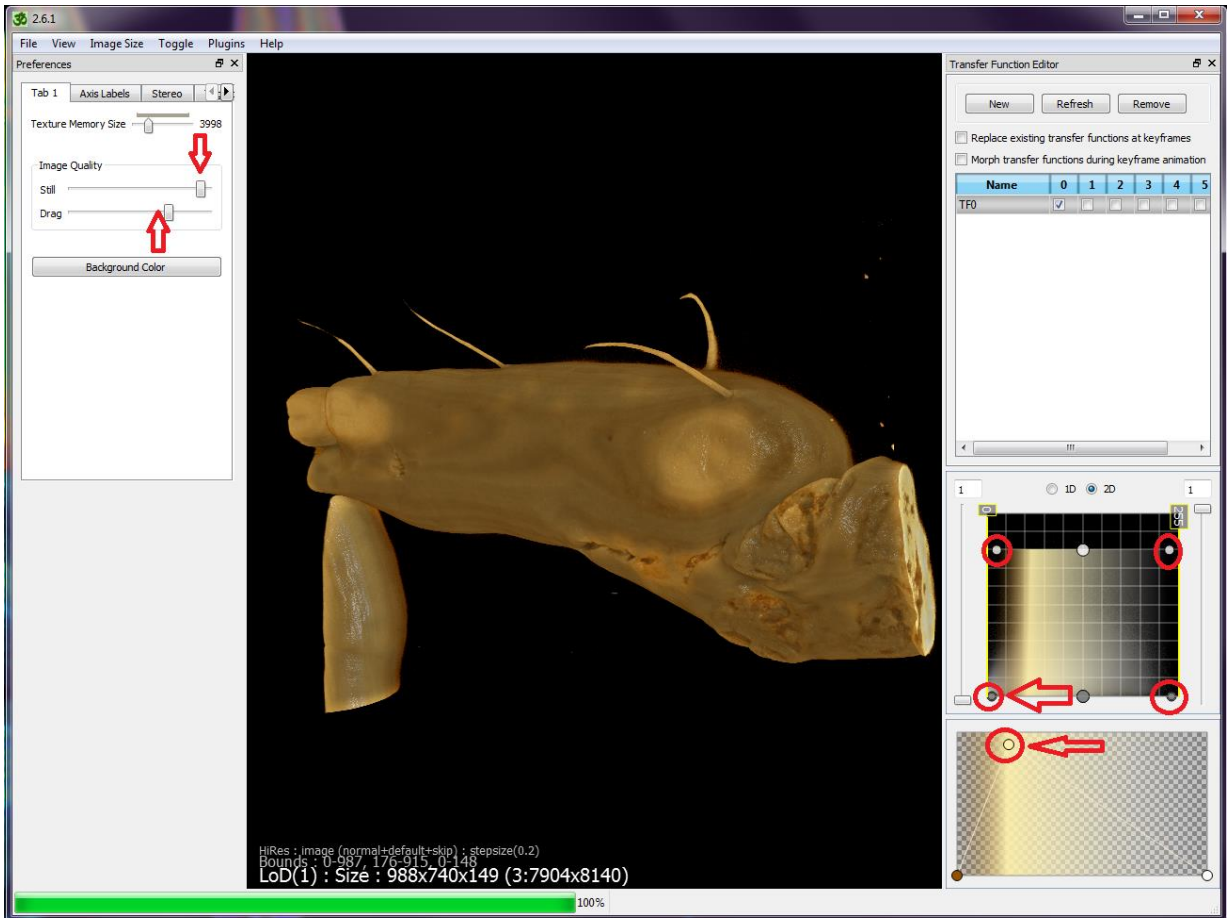

Supp. Fig. 25. Getting high resolution images and some useful tools for Drishti.

To add a scale bar, after opening the command help window by pressing the space bar, the command "scalebar 100" was entered, this applies a 100 µm scale bar to the image (Supp. Fig. 26). To change the location of the scale bar, click and drag it to the correct position.

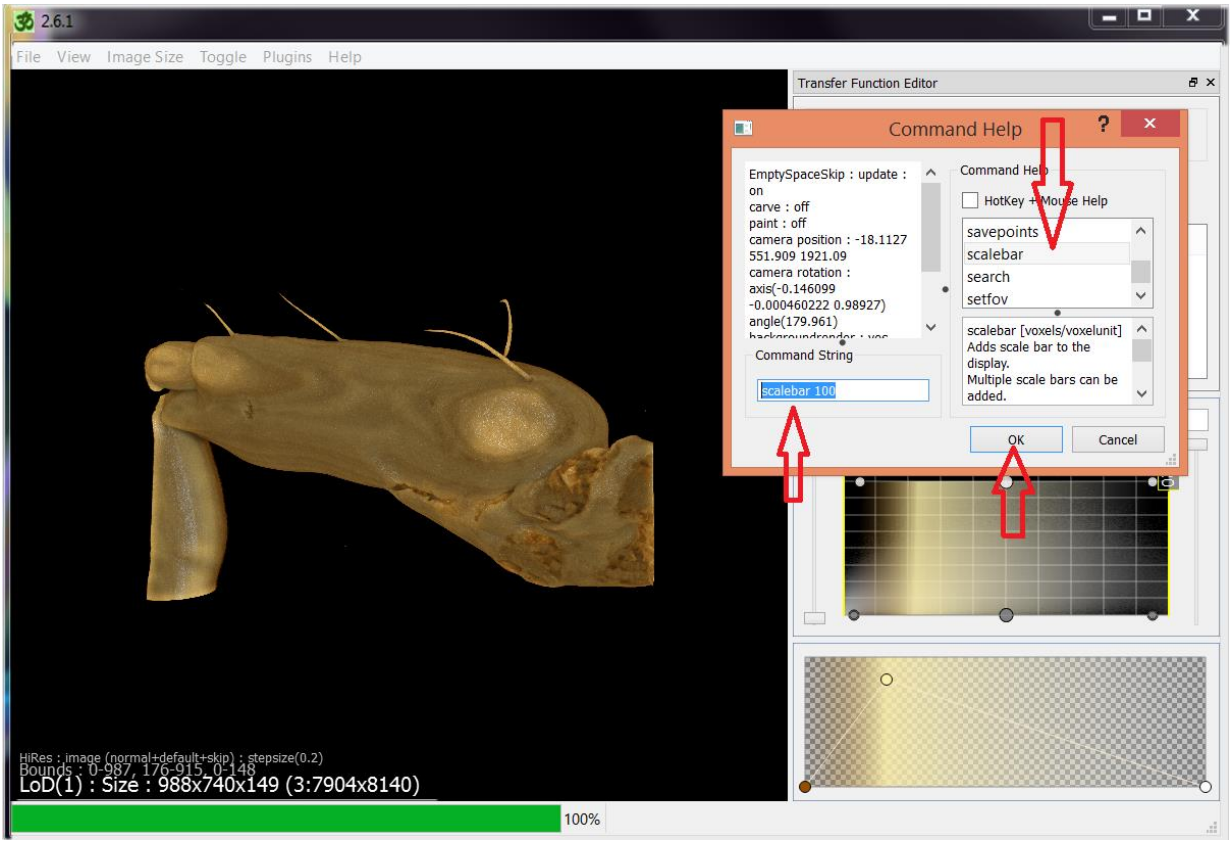

Supp. Fig. 26. Adding a scale bar in Drishti.

The image can be saved by clicking File> Save image (Alt + S); select image size; click OK (Supp. Fig. 27).

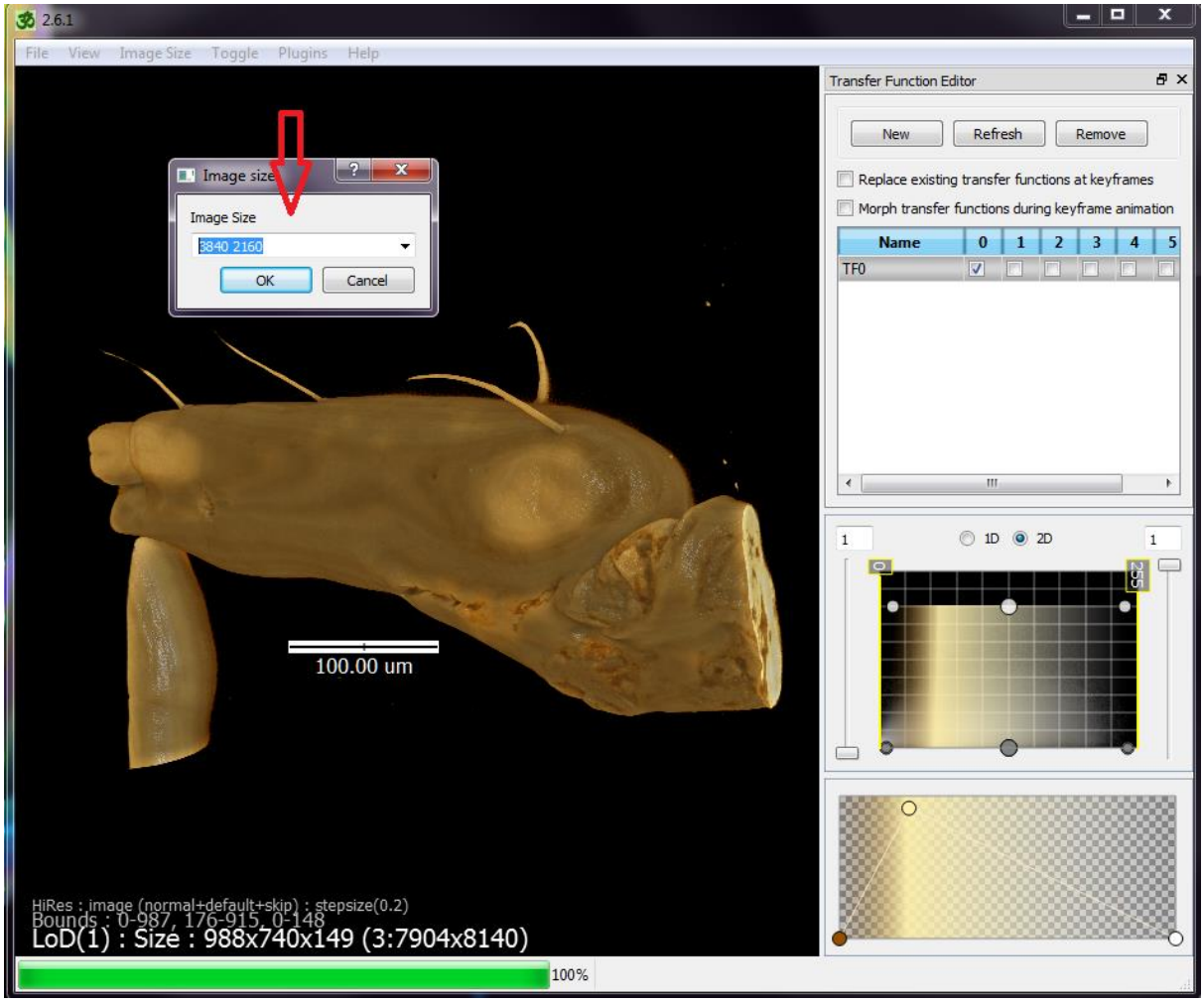

Supp. Fig. 27. Saving the image and selecting image size.

Save snap shots by naming file and type, e.g. MaxillipedII_basis_Drishti.jpg; click Save (Supp. Fig. 28).

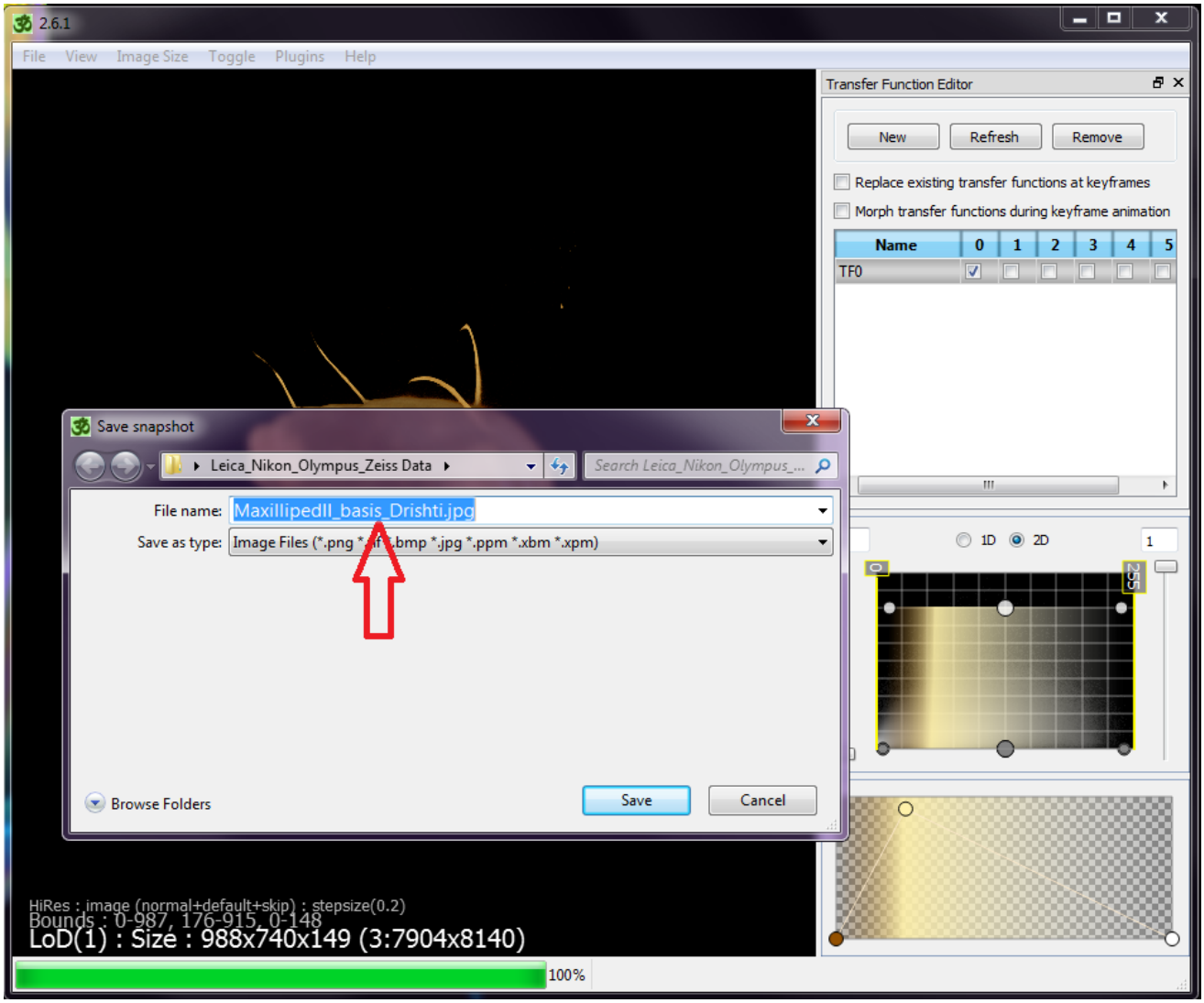

Supp. Fig. 28. Naming image and saving in ***.jpg format.

Select “Mono Image” option in drop down box; click OK. The snapshot will be saved as an image in ***.jpg format (Supp. Fig. 29). The snap shot window will remain open and, the volume can be repositioned and a new snapshot saved.

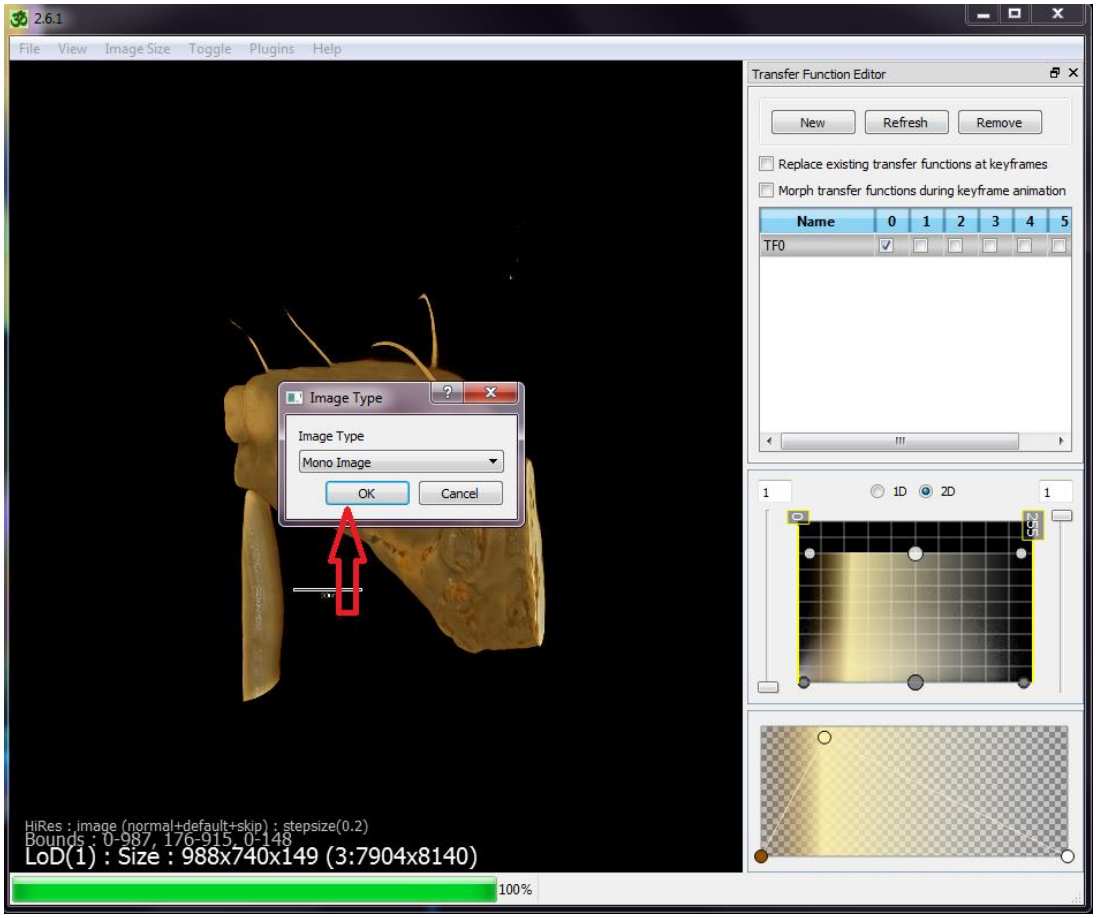

Supp. Fig. 29. Taking a snapshot by selecting Mono Image and saving image.

6. Segmentation instructions

Segmentation is undertaken in high resolution via the F2 key and commences by depressing "spacebar" on keyboard; "Command Help" box appears and select or type "mop update off" in Command String box; click OK (Supp. Fig. 30).

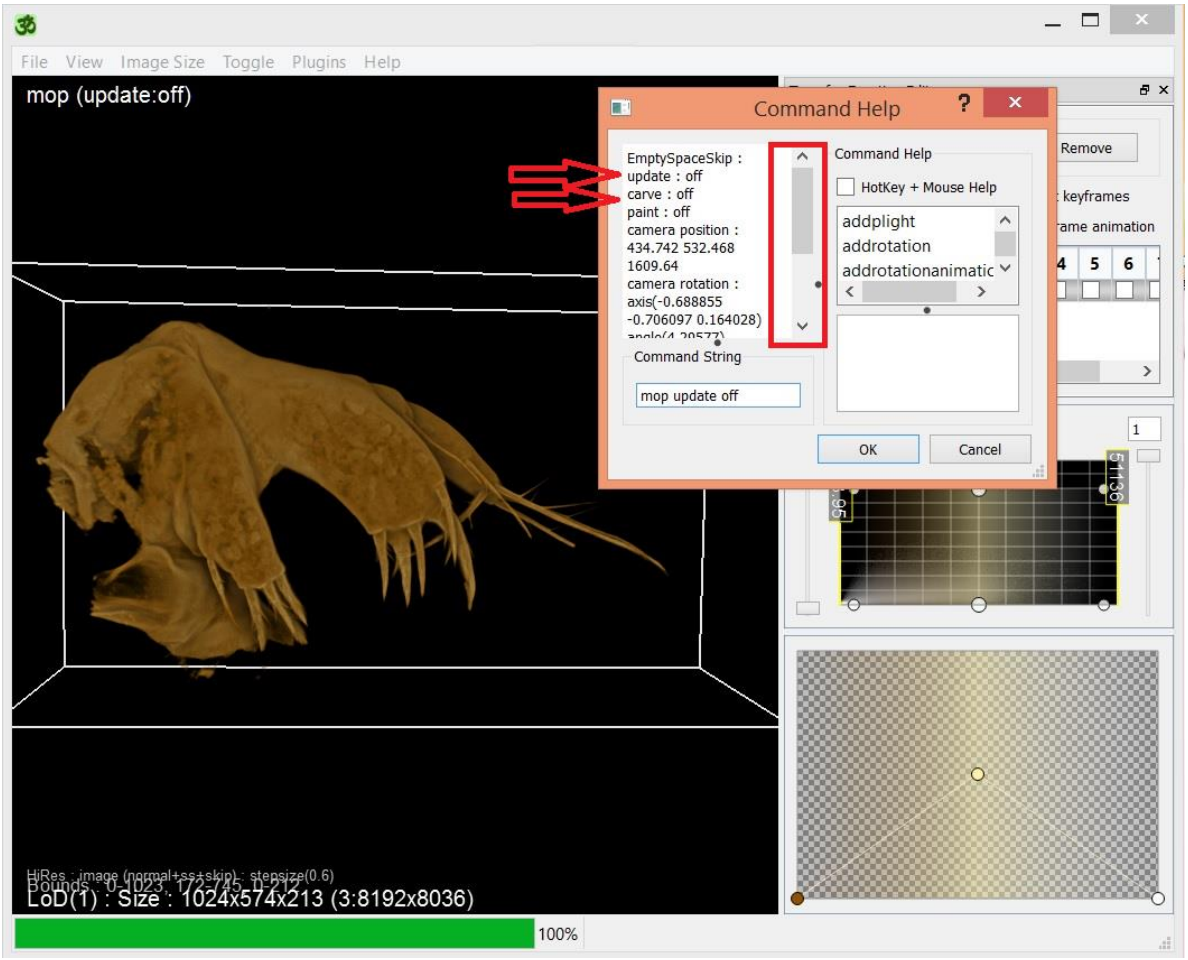

Supp. Fig. 30. Segmentation: selecting mop update off for 3D data using Drishti.

Depress the space bar again and select or type “mop carve” and click OK. Fragments to be removed/deleted can be rotated and cleaned by pressing shift + left click (Supp. Fig. 31). After editing, the procedure can be completed by pressing the space bar again and entering the command “mop carve off”; click OK.

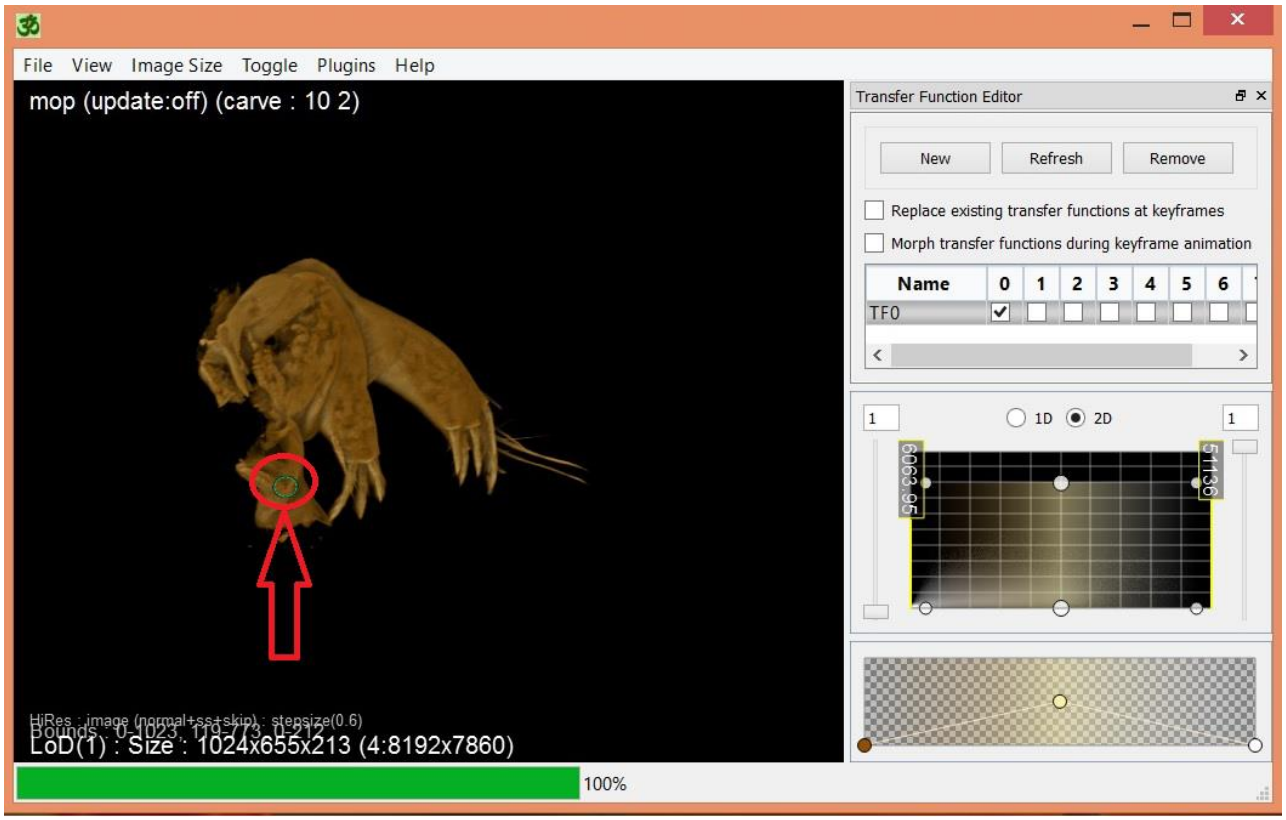

Supp. Fig. 31. Rotating and removal of unwanted fragments in 3D images using Drishti.

Adjusting opacity and colour interface by manipulating the dots (see Supp. Fig. 32). Add scale bar as described above (Supp. Fig. 26).

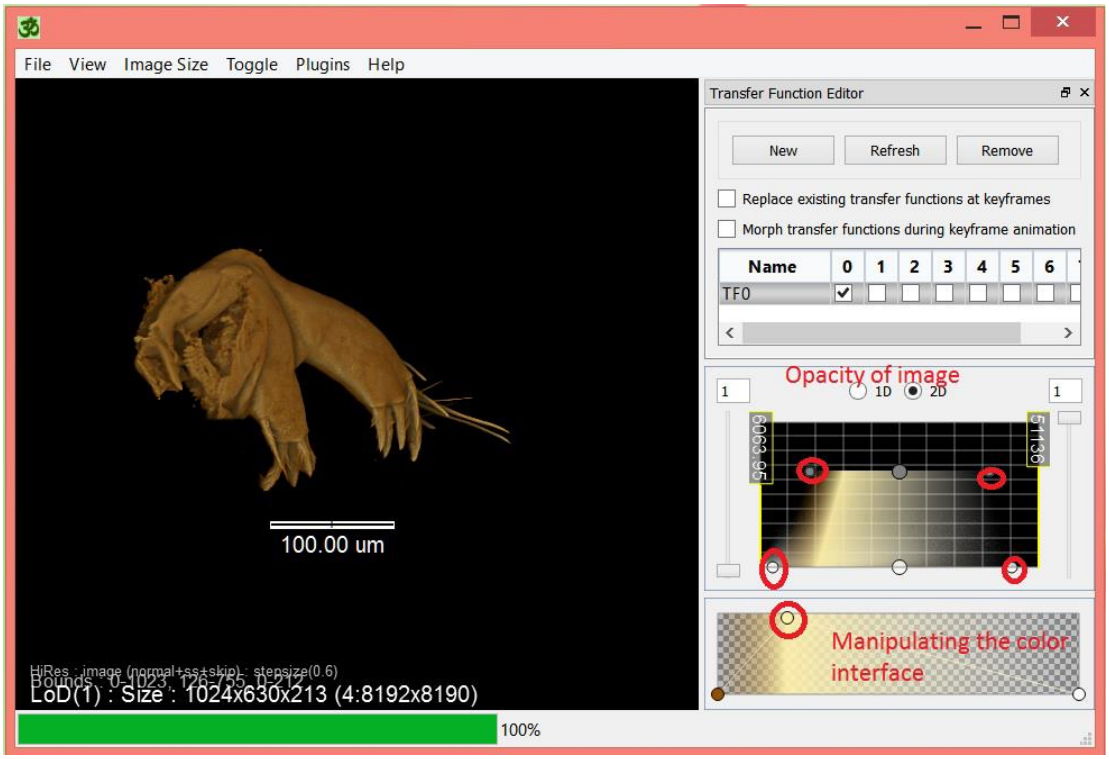

Supp. Fig. 32. Adjusting opacity and colour of the image by manipulating interface.

After the editing process, the image can be saved as "Mono Image" by clicking File> Save image as. If the image is saved as ***.jpg, the background will be black, if ***.tif the background is white.

Table 1. List of reviewed papers that used CLSM in the study of macro-invertebrates with information on studied material, stain, mounting medium, confocal microscope, visualisation and performance observed.

References	Species	Stain	Mounting medium	CLSM	Visualisation*	Performance
Bundy and Paffenhöfer (1993)	*Labidocera aestival*, *Eucalanus pileatus*, *Centropages velificatus* (Copepoda)	DiI (Dioctadecyl-tetramethylindocarbocyanine perchlorate)	Seawater	Biorad MRC600	VoxelView	Optical cross-sections of the specimens can be animated and rotated in 3D.
Galassi *et al*. (1998)	*Moraria poppei*, *Parastenocaris vicesimal* (Copepoda)	Autofluorescence	Polyvinyl lactophenol	Sarastro 2000	Maximum intensity projection (MIP)	CLSM provides better understanding of 3D structure of copepods.
Carotenuto (1999)	*Temora stylifera* (Copepoda)	Autofluorescence	Seawater	Zeiss 410	MIP	A non-destructive and fast method to distinguish transparent copepod stages.

Buttino *et al*. (2003)	*Calanus helgolandicus* (Copepoda, Calanoida), *Hippolyte inermis* (Decapoda)	DiI (Dioctadecyl-tetramethylindocarbocyanine perchlorate)	Seawater	Zeiss 410	Zeiss and Crisel instruments software packages MetaVue	Using bright-field microscopy is time consuming, however, CLSM is an effective method for visualising copepod morphology.
Klaus *et al*. (2003)	*Culex tarsalis, Drosophila melanogaster* (Insecta)	Autofluorescence	Euparal, Glycerine jelly	Zeiss 510	MIP, volume rendering and isosurface rendering	MIP images can be ambiguous. Volume rendered models enhance surface features.
Klaus & Schawaroch (2006)	*Drosophila melanogaster, Culex tarsalis, Cladochaeta inversa* (Insecta)	Autofluorescence	Euparal, Glycerine jelly	Zeiss 510	Zeiss LSM image browser for MIP and Imaris	Using spacer between coverslips protects 3D structure of the specimens. MIP images are good, but Imaris provides more satisfactory visualisation.
Michels (2007)	*Acanthocyclops mirnyi*, *Heterorhabdus* sp., *Alteutha potter* (Copepoda)	Autofluorescence	Euparal, Glycerine jelly	Leica TCS SP5	Amira 3D software	Euparal produces red autofluorescence at excitation

						wavelength of 488nm or less.
						Glycerine jelly is a favourable embedding medium to visualise tiny structures of crustaceans.
Schawaroch & Li (2007)	*Drosophila melanogaster* (Insecta)	Autofluorescence	Glycerine jelly (mixture of mountants)	Zeiss 510	Zeiss LSM image browser for MIP and Imaris	Using agarose with glycerine jelly decreases background noise. Using 3D image re-construction removes low level of background noise.
Valdecasas (2008)	Water mites; *Vagabundia sci* (Axonopsinae (Acari,Parasitengona, Hydrachnidia)	Autofluorescence	Glycerine jelly	Leica TCS SP2	ImageJ	CLSM provides more efficient results than bright field microscope results.
Lee *et al*. (2009)	*Carpatolechia* (Insecta)	Autofluorescence, Mercurochrome, Safranine, Chlorazol black E, Eosin Y,	Euparal	Zeiss LSM 510	MIP	Autofluorescence level of chitin was low. The best results were

		Eosin Y + Chlorazol black E, Orange G				obtained using eosin Y, safranine and mercurochrome respectively. Poor images were obtained using orange-G and eosin Y + chlorazol black E.
Maruzzo *et al*. (2009)	*Artemia* (Crustacea, Branchiopoda, Anostraca)	Evans Blue	Glycerol	Nikon Eclipse E600	MIP	Specimens digested in KOH and stained with Evans Blue provided better results.
Butler *et al*. (2010)	*Ballonema gracilipes* (Chilopoda)	Autofluorescence	Canada balsam	Leica TCS SP1	MIP	Non-destructive imaging for historical museum material. Resolution is comparable to SEM. Canada balsam makes specimens more fluorescent for CLSM visualisation.

Michels & Büntzow (2010)	Small crustaceans and polychaetes	Autofluorescence, Congo red	Glycerine	Leica TCS SP5	Leica LAS software for MIPs	Congo red stains exoskeleton effectively, but internal tissues and proteins were not stained so successfully.
Böhm *et al.* (2011)	*Ionescuellum carpaticum* (Protura, Entognatha Artrophoda)	Autofluorescence	Polyvinyl lactophenol (unstained), Euparal (Congo red)	Leica TCS SP 2	MIP, Fiji, OsiriX	Congo red fades in polyvinyl lactophenol, any mountant such as Euparal can be used so long as it is not strongly autofluorescent.
		Congo red				Autofluorescence of unsclerotised cuticle is low. Stained regions with Congo red was effective.
Menzel (2011)	*Mesocletodes elmari* sp. (Copepoda, Harpacticoida, Argestidae)	Congo red	Glycerol	Leica TCS SP5	MIP	Successful visualisation.
Valdecasas & Abad (2011)	Aquatic mites (Acari, Hydrachnidia)	Autofluorescence	Glycerine jelly	Leica SPE	ImageJ to obtain MIPs, Gamma correction	Using proteinase K does not affect the external morphology of mites.

					with Photoshop CS3	
Brooker *et al*. (2012)	*Lernaeocera branchialis* (Copepoda)	Blankophor, Gomori's trichrome	Distilled water	Leica TCS SP2	Leica Confocal Software (MIP), Photoshop CS3	Successful visualisation.
Brooker *et al*. (2012)	*Lernaeocera branchialis* (Copepoda)	Blankophor, Gomori's trichrome	Distilled water	Leica TCS SP2	LCSM composite images in Photoshop CS3	Using 3D CLSM stack data to draw specimens digitally provides accurate data.
Kihara & Martinez Arbizu (2012)	*Cerviniella danae*, sp. nov., *Cerviniella arctica* sp. nov., *Cerviniella hitoshii* sp. nov. (Copepoda, Harpacticoida)	Congo red	Glycerine	Leica TCS SP5	LAS AF 2.2.1. for MIPs and CLSM illustrations, Adobe Photoshop CS4	For the taxonomic study of new species, CLSM is used to visualise the details of the appendages of the specimens.
Michels & Gorb (2012)	*Locustamigratoria*,*Sympetrum striolatum*, *Eristalis tenax* and so on (Insecta), *Temora longicornis* (Copepoda)	Autofluorescence, Congo red	Glycerine	Zeiss LSM 700	ZEN software	CLSM is a good tool to visualise resilin in arthropods. It is also effective to detect the differences in the material composition.

Michels *et al*. (2012)	*Centropages hamatus* (Copepoda)	Congo red, Fluorescein isothiocyanate	Glycerine	Zeiss LSM 700	Nikon Capture NX 2, Adobe Photoshop CS4	Successful visualisation.
Brandt *et al*. (2014)	*Atlantoserolis vemae* (Isopoda: Serolidae)	Congo red and acid fuchsin	Glycerine	Leica TCS SPV	LAS AF 2.2.1. for MIPs and CLSM illustrations, Adobe Photoshop CS4	Stained whole specimen and the dissected parts (e.g. mouthparts and legs) were visualised using CLSM.
Kaji *et al*. (2014)	Clam shrimp (Crustacea, Branchiopoda)	Rhodamine, Phalloidin	Vectashield	Leica TCS SP5 II	Imaris	The cuticle surface is smooth and fine setae are present using Imaris.
Dreszer *et al*. (2015)	*Cyphophthalmus solentiensis* sp. nov. (Arachnida)	Autofluorescence	Glycerine	Zeiss Elyra	Carl Zeiss Zen software	Successful visualisation by taking advantage of the autofluorescence of the arthropod cuticle.
Wilkommen *et al*. (2015)	*Ischnura elegans* (Insecta)	Autofluorescence	Glycerine	Zeiss LSM 700	ZEN 2009 for MIPs	Successful visualisation.

*Some of the papers did not provide detailed information on visualisation.

Please click link below to find paper photos with original sizes:
https://www.dropbox.com/sh/lopvjnhr0parn96/AADIv0T4S76hnqU3QWlGAa8La?dl=0

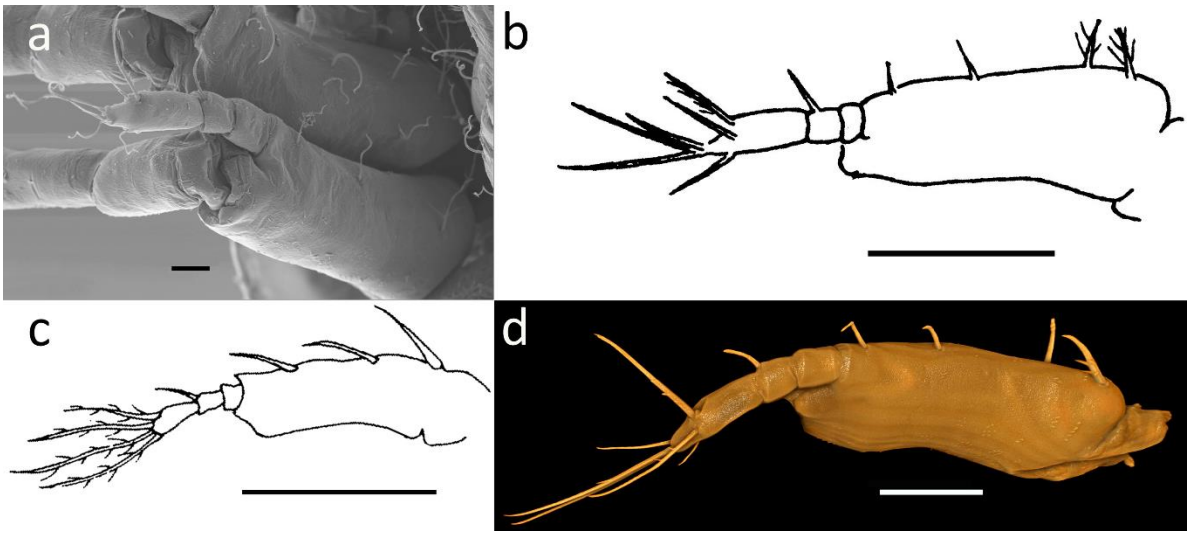

Fig. 1. *Eriocheir sinensis*, zoea I, second maxilliped. A comparison of (a) SEM image obtained using Zeiss Ultra Plus Field Emission. (b) Line drawing from Kim & Hwang (1995). (c) Line drawing from Montu *et al*. (1996). (d) Drishti image obtained using Nikon A1-Si CLSM. Scale bars a = 20 μm; b-d = 100 μm.

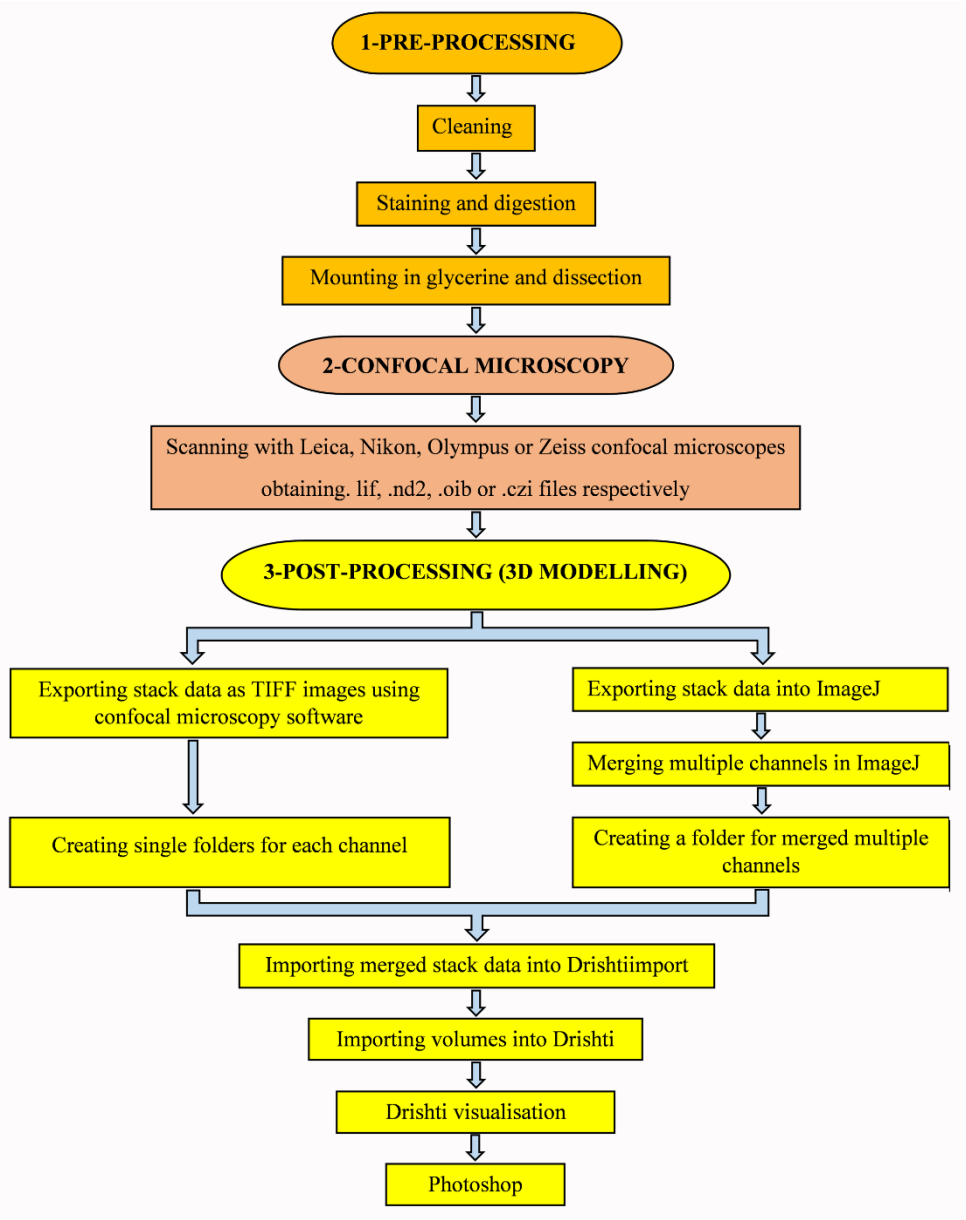

Fig. 2. A flowchart for visualisation and 3D imaging of brachyuran crab larvae.

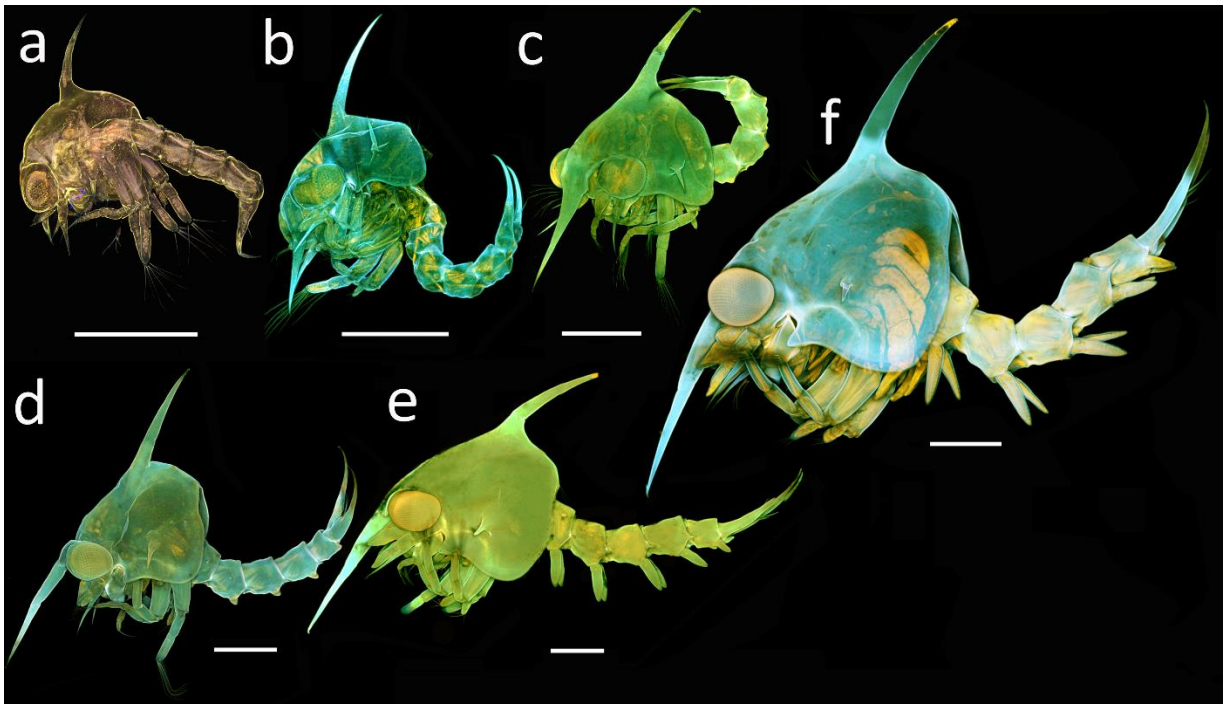

Fig. 3. *Eriocheir sinensis* zoeal stages using Nikon A1-Si CLSM. Confocal images. (a) ZI, 10× dry objective. (b) ZII, 10× dry objective applying "large images" option, scan area of 2×1 fields for image stitching. (c) ZIII, 10× dry objective applying "large images" option, scan area of 2×2 fields for image stitching. (d) ZIV, 10× dry objective applying "large images" option, scan area of 3×2 fields for image stitching. (e) ZV, 10× dry objective applying "large images" option, scan area of 4×3 fields for image stitching. (f) ZVI, 10× dry objective applying "large images" option, scan area of 4×4 fields for image stitching. Scale bars = 500 μm.

Fig. 4. Preparation of slide using reinforcement rings.

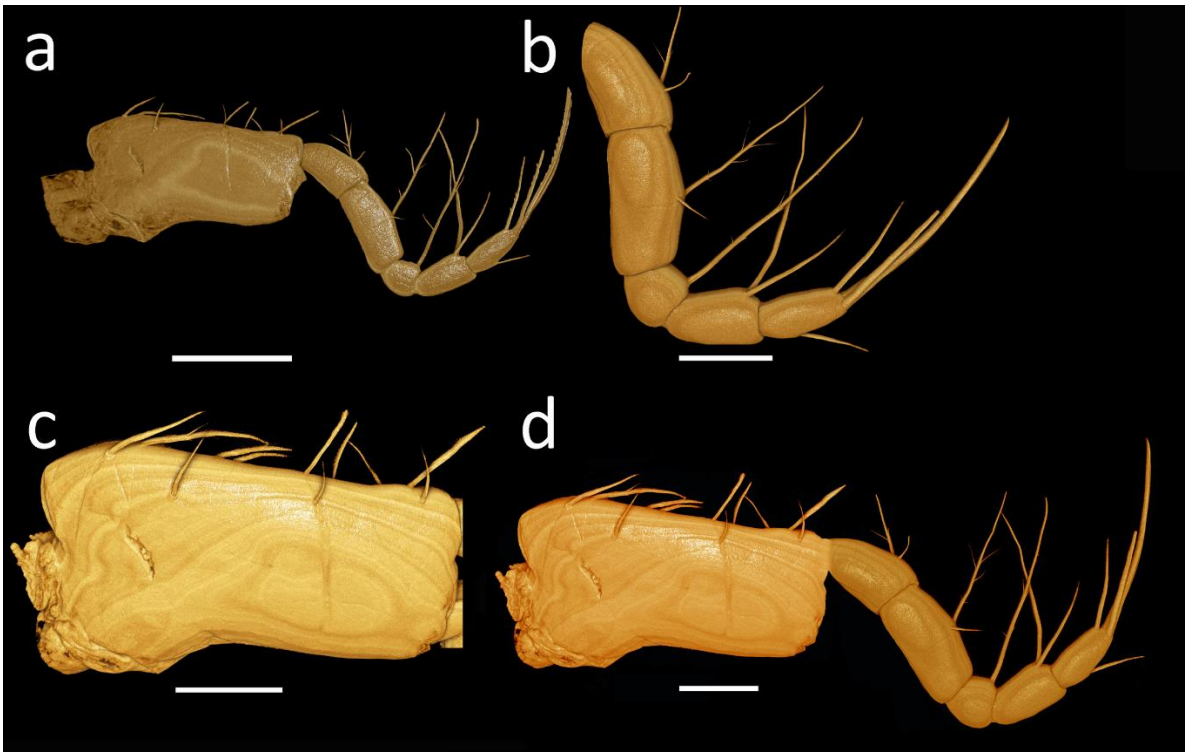

Fig. 5. *Eriocheir sinensis*, zoea II, Drishti images of first maxilliped using Nikon A1-Si CLSM. (a) Basis and endopod, scan area of 1×2 fields for image stitching, 20× dry immersion objective applying "large images" option. (b) Endopod. (c) Basis. Both using 40× oil immersion objective. (d) Basis and endopod merged from two images using Adobe Photoshop, after applying ImageJ and Drishti. Scale bars a = 300 µm; b-d = 100 µm.

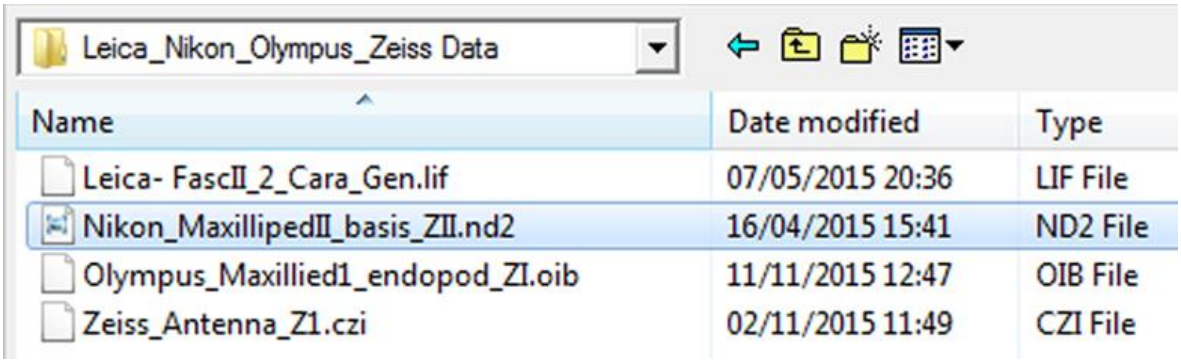

Fig. 6. File formats of different confocal microscopes. Leica uses ***.lif files. Nikon uses ***.nd2 files. Olympus uses ***.oib files. Zeiss uses ***.czi files.

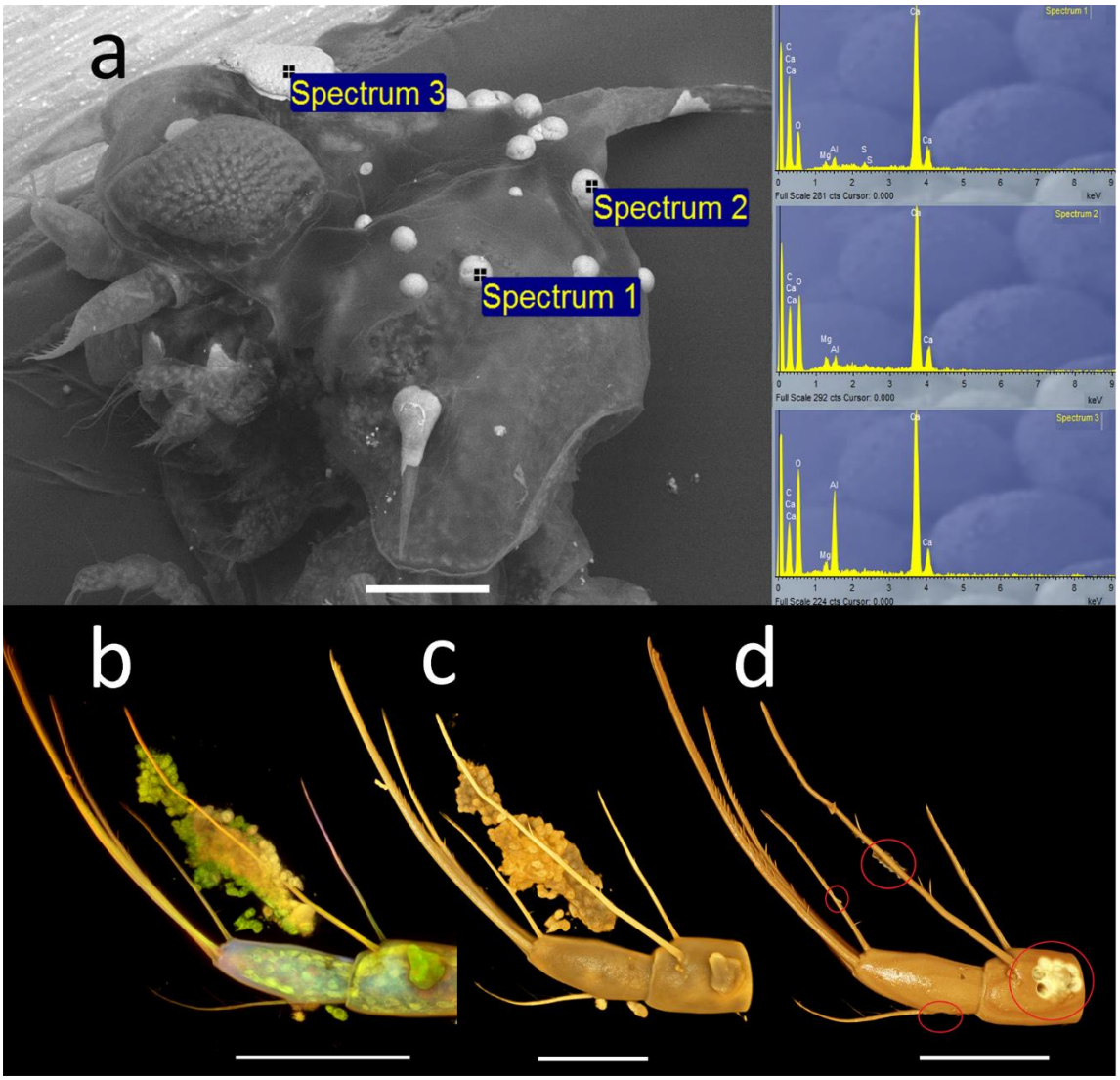

Fig. 7. *Eriocheir sinensis*, zoeae with debris adhered to the exoskeleton. (a) ZI showing calcium carbonate using SEM LEO 1455 VP analysis. (b) ZII, confocal image of endopod using Nikon A1-Si CLSM, 60× oil immersion objective. (c) ZII, Drishti image of endopod. (d) ZII, attempt at debris removal using Drishti and Photoshop was not always successful, see circled areas. Scale bars a = 300 µm; b-d= 100 µm.

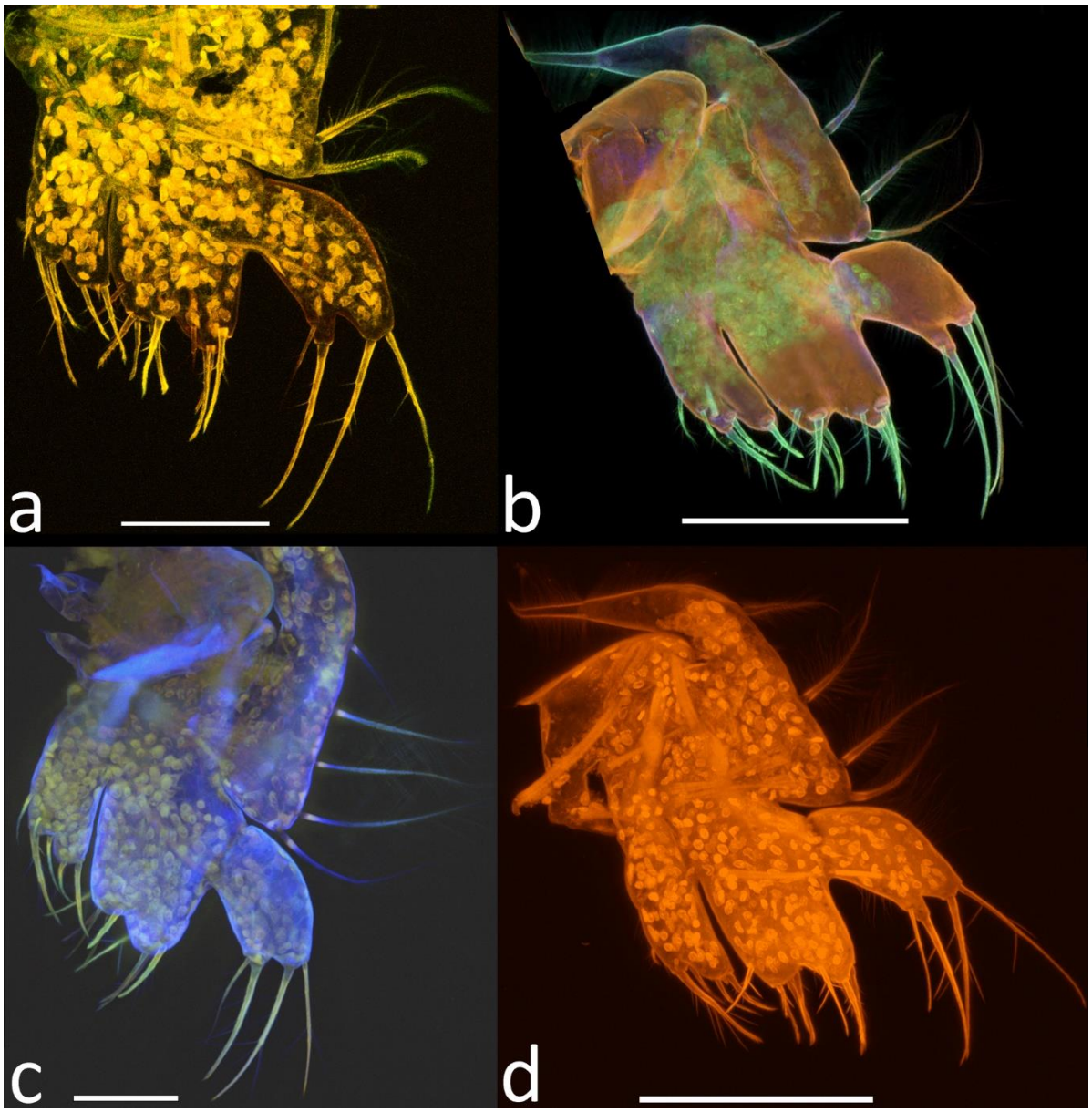

Fig. 8. Advantages of staining and digesting appendages. *Eriocheir sinensis*, zoea I, scanned images of the maxilla using Nikon A1-Si CLSM. (a) Undigested and unstained, 60× oil immersion objective. (b) Digested and stained with Congo red and acid fuchsin, 40× oil immersion objective. (c) Undigested and stained using only Congo red, 60× oil immersion objective. (d) Undigested and stained using the mixture of Congo red and acid fuchsin, 40× oil immersion objectives. Scale bars a, c = 50 μm; b, d = 100 μm.

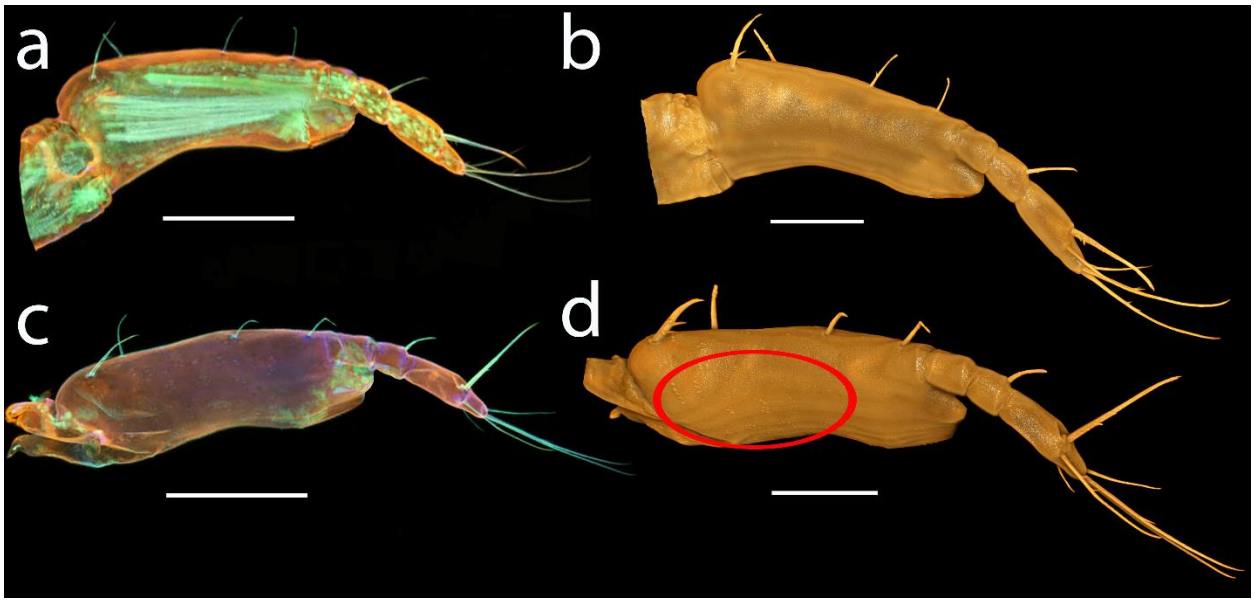

Fig. 9. Advantages of digesting appendages. *Eriocheir sinensis*, zoea I, images of second maxilliped using Nikon A1-Si CLSM. (a) Confocal image of non-digested appendage showing basial musculature. (b) Drishti image of non-digested appendage. c) Confocal image of digested basial muscles. (d) Drishti image of digested appendage (tiny structures are circled). All 40× oil immersion objective, applying "large images" option, scan area of 1×2 fields for image stitching. Scale bars = 100 μm.

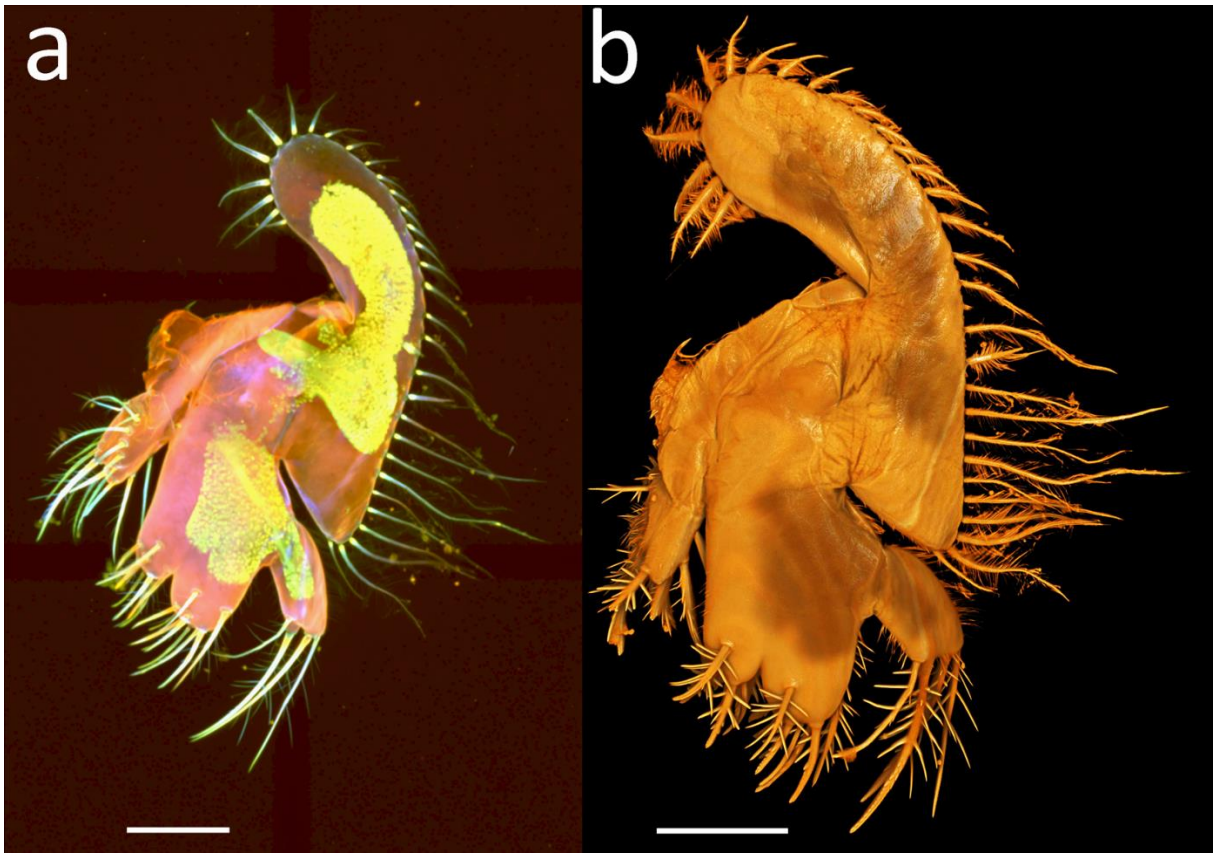

Fig. 10. "Tiling" appendages when scanning at higher magnification. *Eriocheir sinensis*, zoea V, image of maxilla using Nikon A1-Si CLSM. (a) Confocal image showing tiled areas. (b) Drishti image. 40× oil immersion objective, applying "large images" option, scan area of 2×3 fields for image stitching. Scale bars a = 100 μm; b = 200 μm.

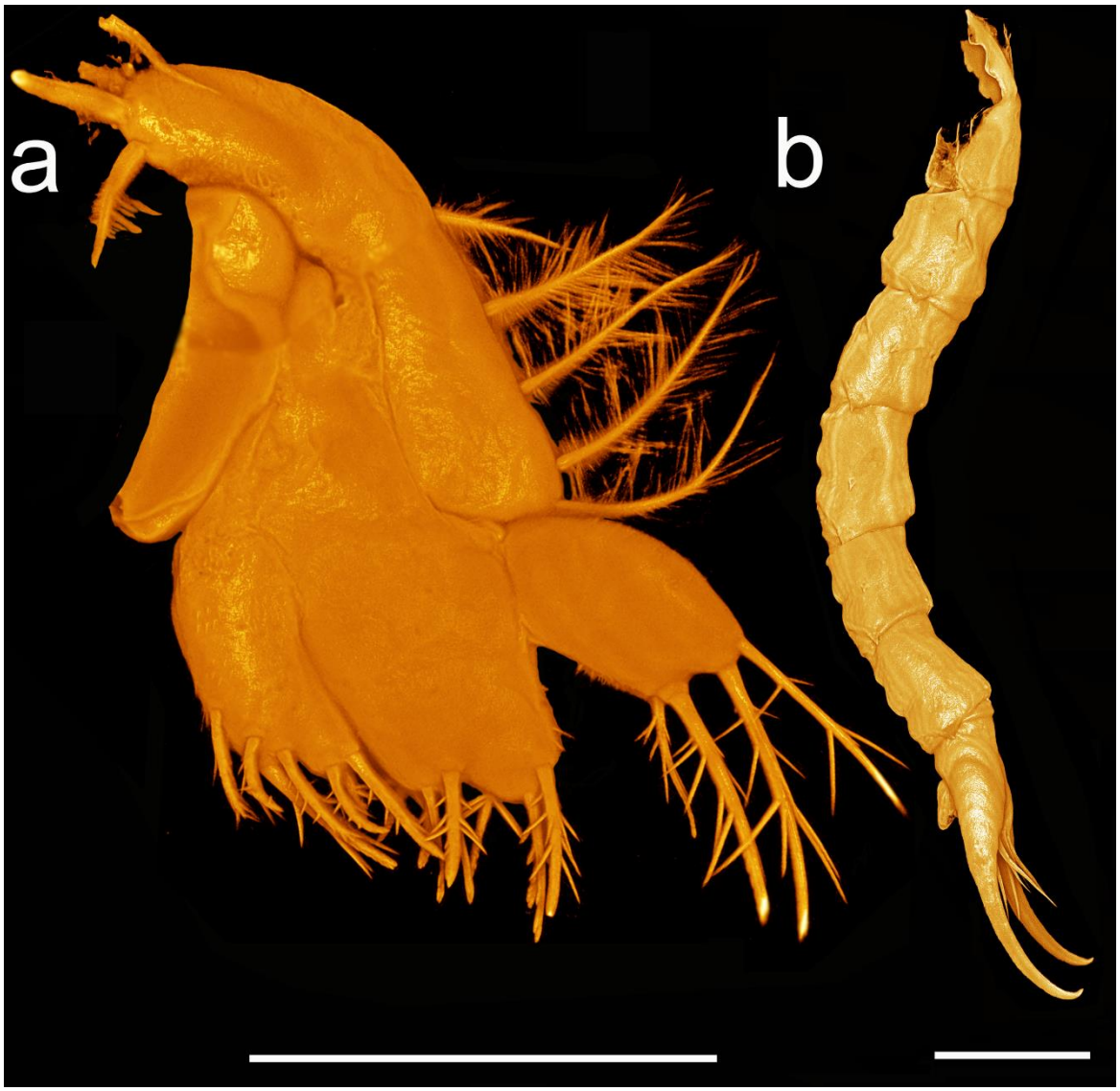

Fig. 11. Merging Drishti images using Adobe Photoshop. *Eriocheir sinensis* zoeal appendages using Nikon A1-Si CLSM. (a) ZII, maxilla, 40× oil immersion objective. (b) ZI, lateral view of pleon, 20× dry immersion objective. Scale bars a = 200 μm; b = 300 μm.

Fig. 12. Visualisation of fine setae. *Eriocheir sinensis*, zoea I. Image of dorsal view of pleon using Nikon A1-Si CLSM, 40× oil immersion objective, applying "large images" option, scan area of 2×6 fields for image stitching. Scale bar = 200 μm.

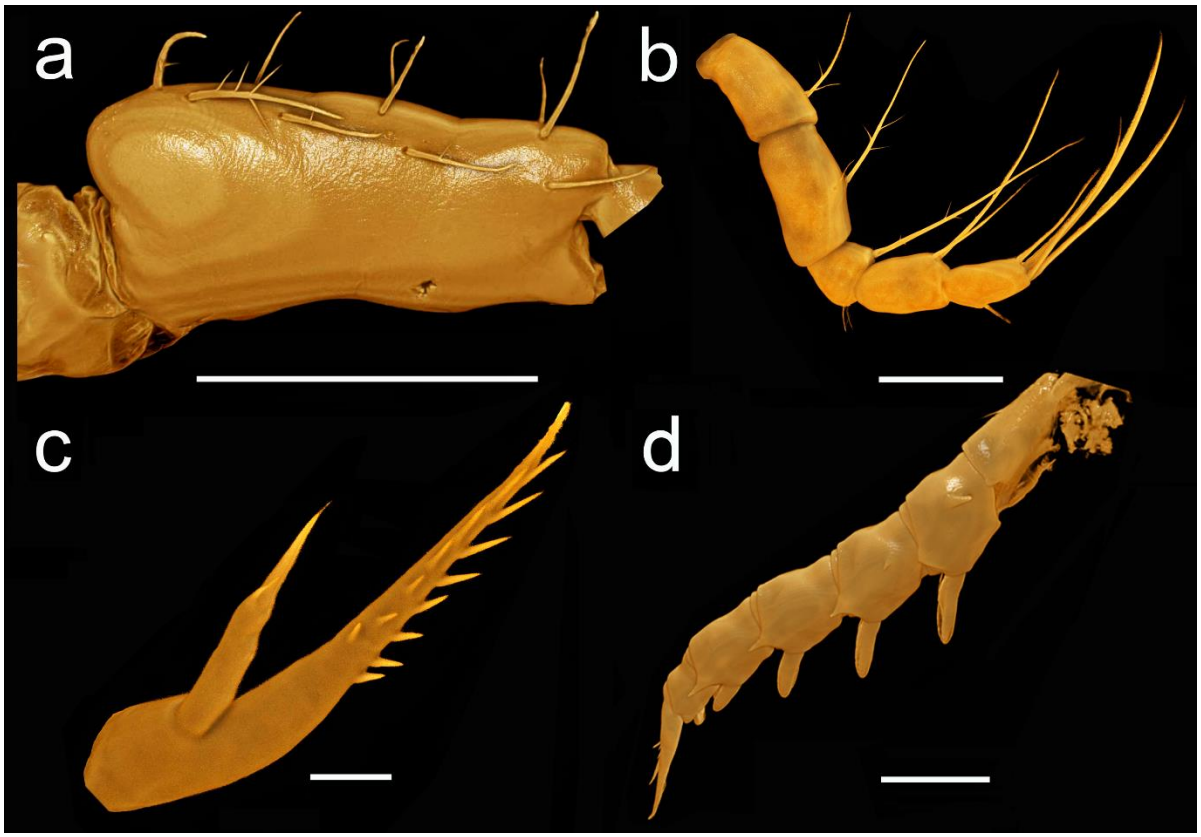

Fig. 13. Scanned brachyuran crab larvae using different brands of CLSM processed in Drishti. *Eriocheir sinensis*, zoea I, first maxilliped. (a) Basis, Nikon A1-Si CLSM. (b) Endopod, Olympus Fluoview FV1000 IX8. (c) Antenna, Zeiss LSM 880 airy scan. All 40× oil immersion objective. (d) *Sesarma curacaoense*, ZIV, lateral view of pleon, Leica TCS SP5, 10× dry objective. Scale bars a-b = 100 µm; c = 50 µm; d =500 µm.

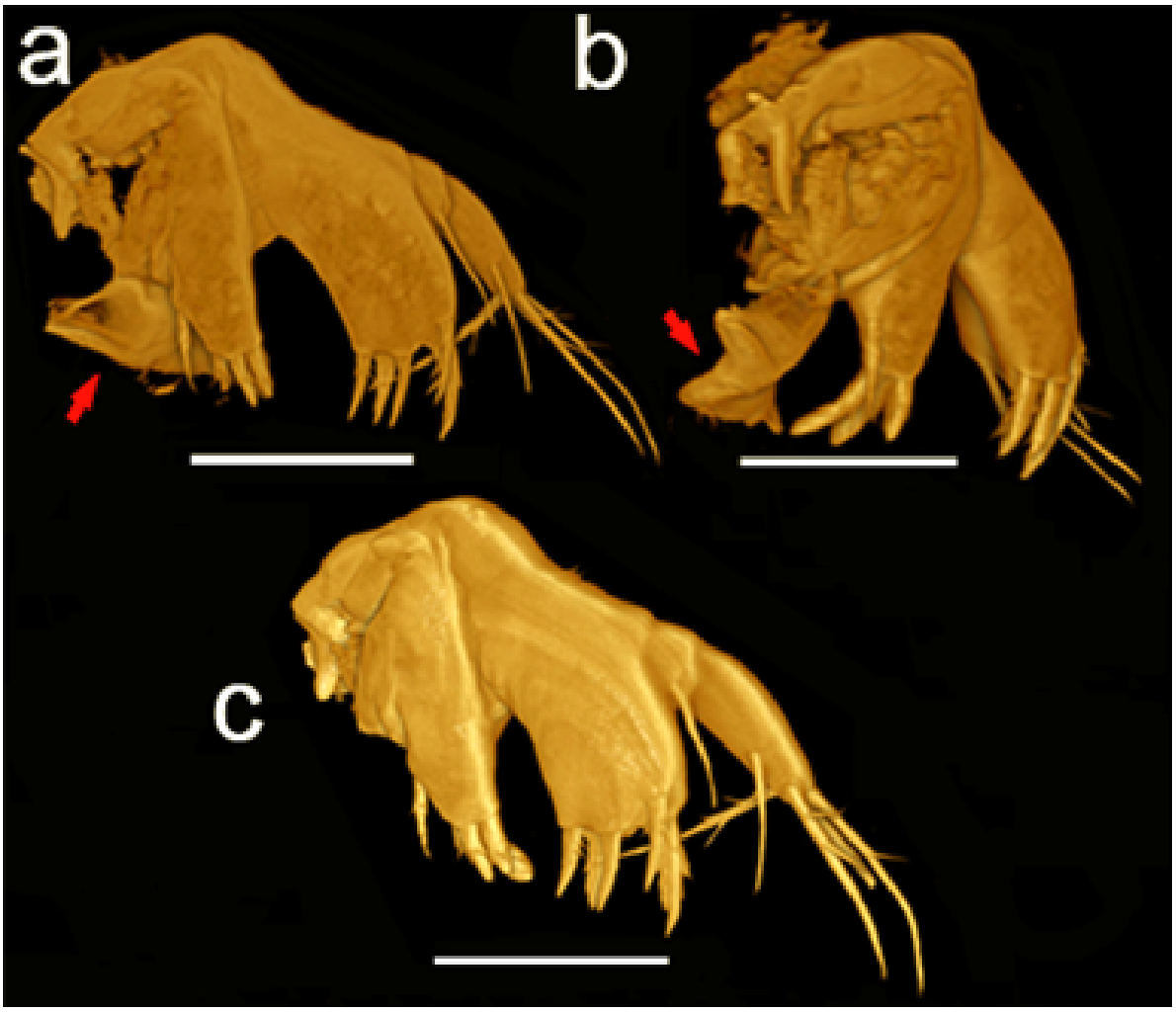

Fig. 14. Digital dissection. *Eriocheir sinensis*, zoea I, image of maxillule using Nikon A1-Si CLSM and processed using Drishti. (a) Unwanted tissue arrowed. (b) Repositioning of appendage to allow the removal of unwanted tissue (arrowed). (c) After digital dissection of tissue (compare a with c). 40× oil immersion objective. Scale bars = 100 μm.

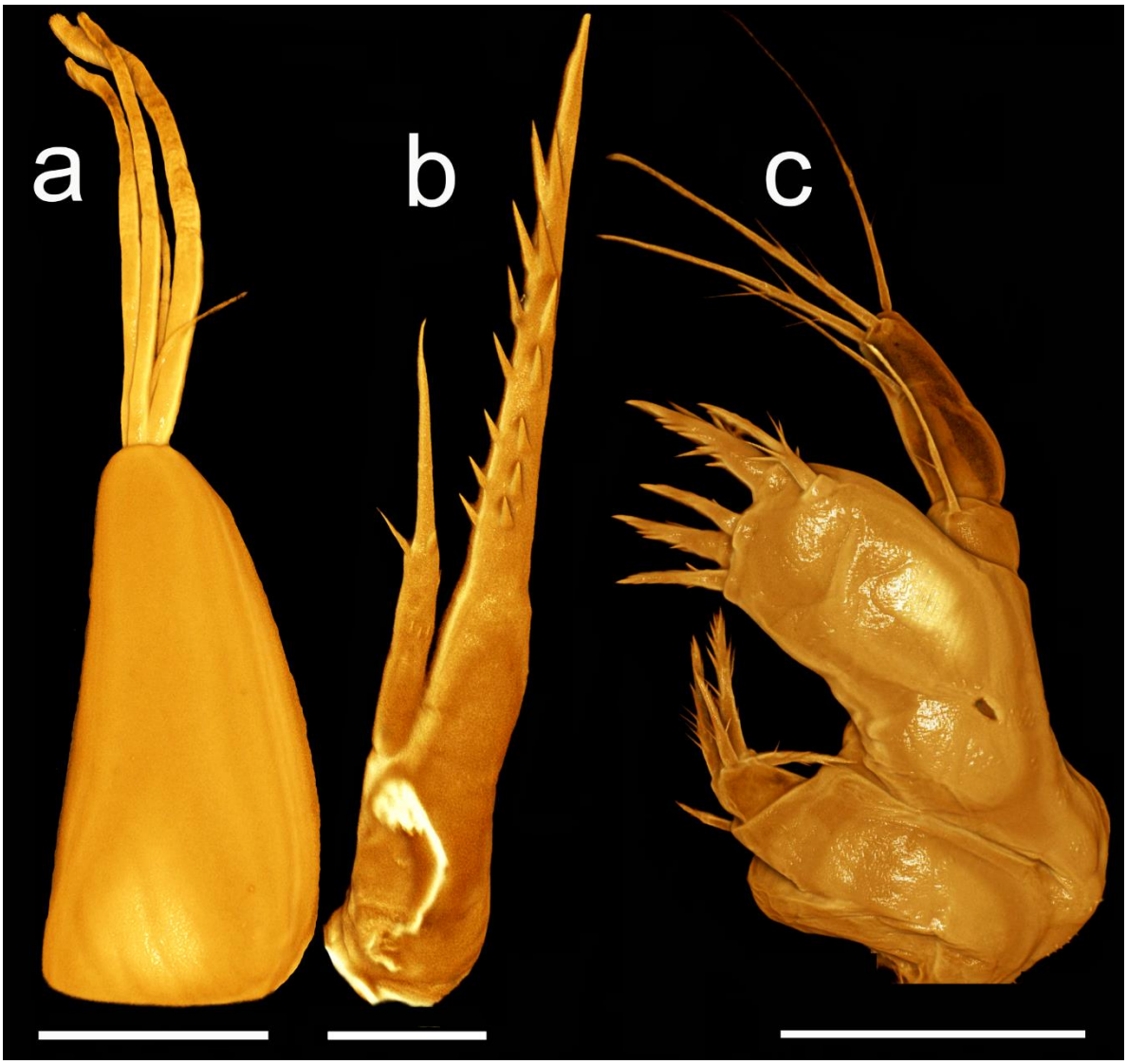

Fig. 15. Drishti images of *Eriocheir sinensis* zoeal appendages using Nikon A1-Si CLSM: (a) ZII, antennule, 40× oil immersion objective. (b) ZI, antenna, 60× oil immersion objective. (c) ZI, maxillule, 40× oil immersion objective. Scale bars a, c = 100 μm; b = 50 μm.

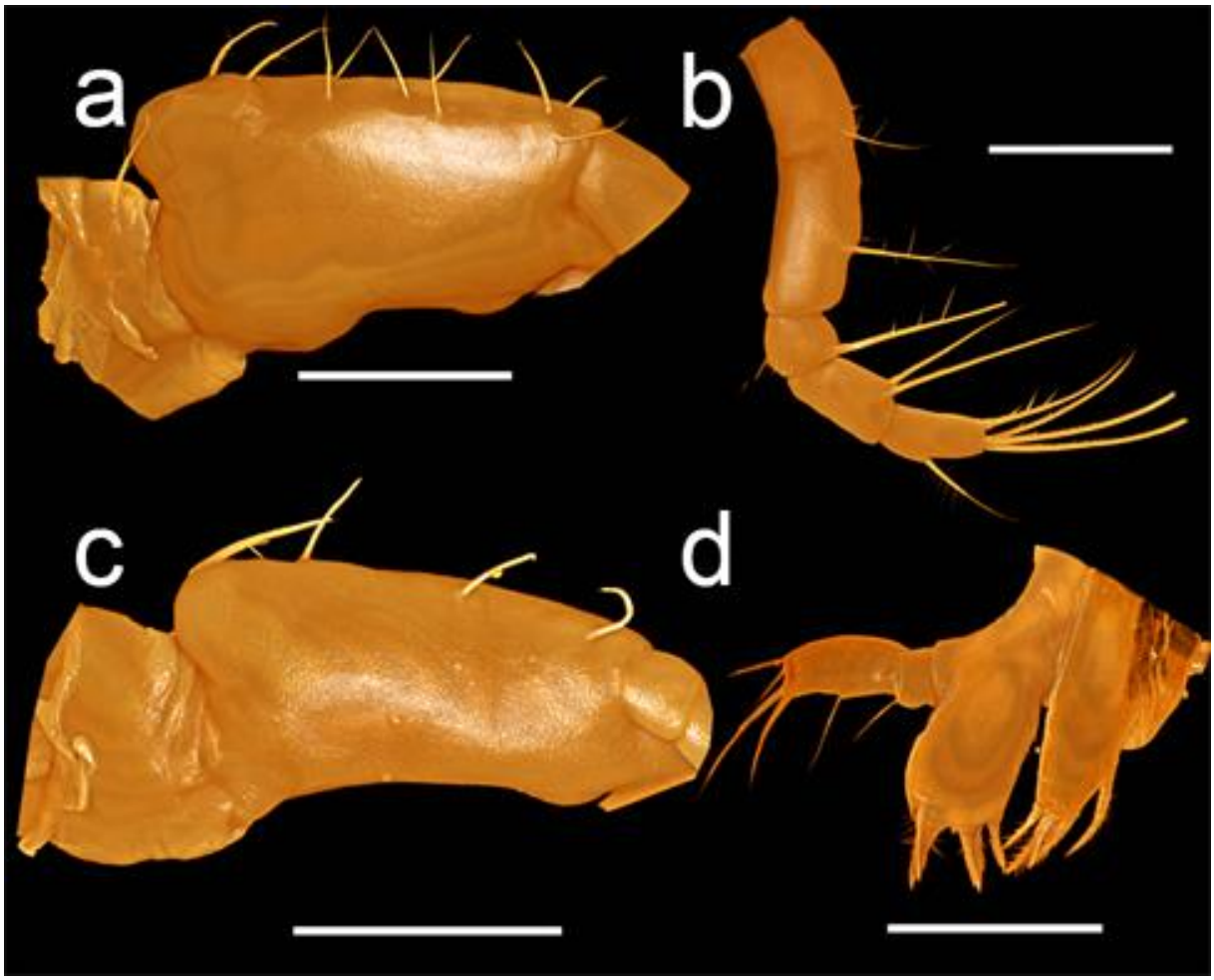

Fig. 16. Drishti images of *Sesarma curacaoense*, zoea I appendages using Leica TCS SP5. First maxilliped. (a) Coxa and basis. (b) Endopod. (c) Coxa and basis of second maxilliped. (d) Maxillule. All 40× oil immersion objective. Scale bars a-b = 50 μm; c-d = 100 μm.

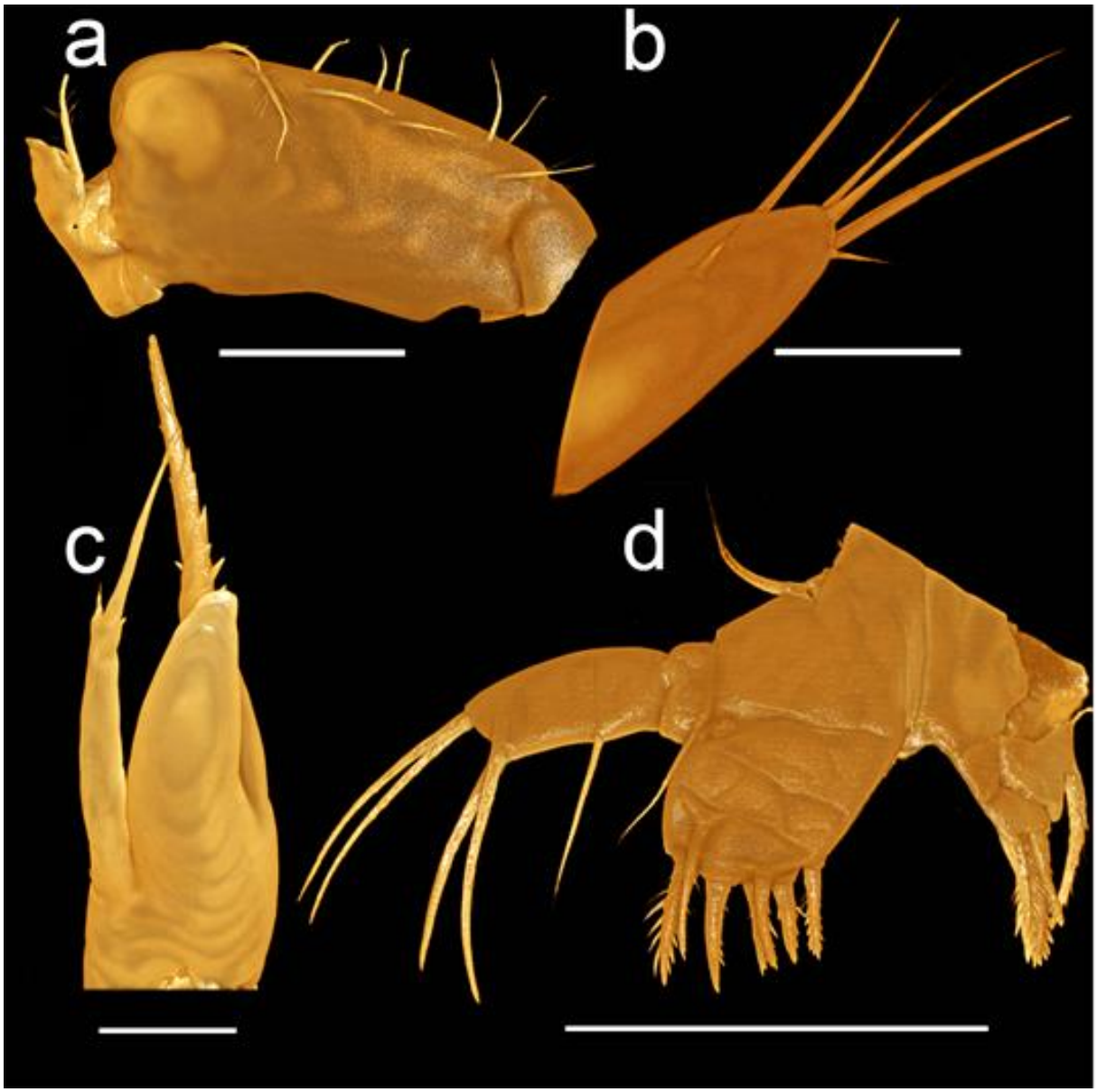

Fig. 17. Drishti images of *Armases miersii*, zoea IV appendages using Leica TCS SP5. (a) Coxa and basis of first maxilliped. (b) Endopod of second maxilliped. Both using 40× oil immersion objective. (c) Antenna. (d) Maxillule. Both using 20× dry objective. Scale bars a, d = 200 μm; b-c = 100 μm.

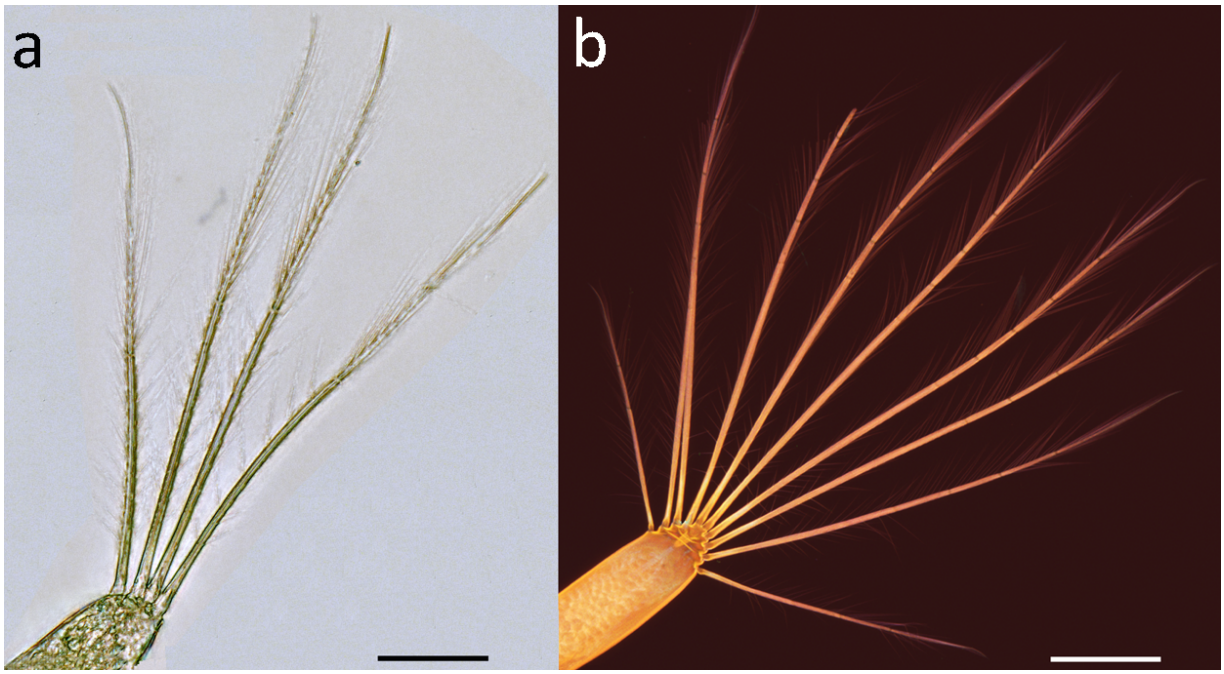

Fig. 18. Comparing bright field and confocal images. *Eriocheir sinensis* zoea, images of second maxilliped using Nikon A1-Si CLSM. (a) ZI, bright field image of exopod, 20× dry objective. (b) ZIV, confocal image of exopod, 20× dry objective applying "large images" option, scan area of 1×2 fields for image stitching. Scale bars a = 50 μm; b = 100 μm.